AN ABSTRACT OF THE THESIS OF

William James Grenney (Name) for the Master of Science (Degree)

in Civil Engineering (Major) presented on Oct. 16, 1970 (Date)

Title: MODELING ESTUARY POLLUTION BY COMPUTER SIMULATION

Abstract approved: Redacted for privacy

Dr. David A. Bella

A digital computer model was developed to simulate the time and space distribution of a dissolved pollutant in an estuary. The program is basically a one-dimensional finite-difference model, but two dimensions can be represented by attaching together several one-dimensional channels. The influence of convection, dispersion and decay are included in the model. The time scale is based on increments of less than one tidal cycle so that intertidal velocities are represented.

A sensitivity analysis was conducted on the convection portion of the model and several tables and graphs are included to indicate the nature and magnitude of numerical errors associated with the model. A method for correcting these errors is also presented.

A tracer study was conducted on the Yaquina Estuary, Newport, Oregon and results are compared with two computer model simulations.

Modeling Estuary Pollution by Computer Simulation

by

William James Grenney

A THESIS

submitted to

Oregon State University

in partial fulfillment of
the requirements for the
degree of

Master of Science

June 1971

APPROVED:

Redacted for privacy

Assistant Professor of Civil Engineering

in charge of major

Redacted for privacy

Head of Department of Civil Engineering

Redacted for privacy

Dean of Graduate School

Date thesis is presented Oct 16, 1970

Typed by Barbara Eby for William James Grenney

ACKNOWLEDGEMENT

The writer gratefully acknowledges the financial assistance of the Federal Water Quality Control Administration for the research support and the traineeship which enabled the writer to pursue graduate study at Oregon State University.

Professor Donald C. Phillips and Assistant Professors Bard Glenne and Peter C. Klingeman are thanked for their comments and help during the entire research project.

Special thanks are due Assistant Professor David A. Bella for his confidence and helpful assistance as major professor.

Grateful appreciation is expressed to my wife, Sally, for her patience and inspiration during the year of study.

TABLE OF CONTENTS

LIST OF FIGURES

LIST OF TABLES

MODELING ESTUARY POLLUTION BY COMPUTER SIMULATION

INTRODUCTION

The rapid population expansion and resultant urban and industrial growth have caused vast increases in the quantities of waste materials being produced. Even if advanced treatment facilities were available to process these waste loads, the effluent would still contain sufficient dissolved materials or heat to influence the ecology of receiving water bodies. The expanding population also means increased requirements for safe and aesthetic aquatic environments, especially in the vicinity of population centers. For these reasons, predicting the impact of domestic and industrial wastes on the aquatic environment remains one of the most urgent problems facing the sanitary engineer.

Estuaries are among the most complex of all disposal sites. They are characterized by irregular geometry, unsteady flow and a blending of chemical, biological, meteorological and hydraulic interactions. Due to the complexity of the system, it often becomes necessary to consider only the principle mechanisms influencing the pollutant distribution in order to simplify the problem to one of manageable terms. The most significant simplifying assumption, and the one that has been almost universally applied, is that of one-dimensional flow in the channel or in a finite segment of the channel. The basic

equation describing a non-conservative pollutant in a one-dimensional channel is derived from mass balance considerations on a differential element and can be expressed as:

$$\frac{\partial(AC)}{\partial T} = \frac{\partial}{\partial x}\left(AD\frac{\partial C}{\partial x}\right) - \frac{\partial(UAC)}{\partial x} - KAC \qquad (1)$$

where C = pollutant concentration, T = time, x = distance along the channel, A = cross section area, D = longitudinal dispersion coefficient, U = average velocity over the cross section, and K = decay constant. The first term on the right-hand side of Equation 1 is the dispersion term and represents the transport of material due to non-uniform velocity gradients in the stream profile. The second term represents convection of the material and the third term represents first-order biochemical decay.

PURPOSE AND SCOPE

Predicting the fate of pollutants in estuaries has been the object of a large research effort during the past decade. A wide variety of models have been developed during this period and the results compared to observed data from the prototype with varying degrees of success. Many of these models utilize numerical methods which are subject to subtle and sometimes unobserved numerical errors. Associated with these studies is the major problem of describing the hydraulic regime so that proper flow velocities can be applied to the convection term in the model.

The present study was undertaken to refine one type of finite-difference model by developing an efficient means of predicting stream velocities and by correcting numerical errors introduced by the difference approximation of Equation 1.

A computer program was written to describe the fate of a dissolved pollutant in an estuary. The dispersion, convection and decay relationships in the model are based on finite-difference methods described by Bella and Dobbins (1968).

The prediction of water surface elevations is based on the propagation of a tidal wave upstream from the mouth of the estuary. Stream flows are determined from changes in water surface elevations by finite-difference methods. Numerical errors associated with the

convection term of the model are analyzed in detail. The model is used to simulate the buildup of a pollution concentration in the vicinity of an outfall during slack waters. Results are compared to a tracer study on the Yaquina Estuary, Newport, Oregon.

LITERATURE REVIEW

General

Two distinctly different types of time scales are used in estuary modeling. One is a time scale such that velocity variation caused by tidal action are included directly in the model, and thus, the pollutant distribution is a function of tidal elevations. In these models, concentrations in the channel can be calculated at any time during a tidal cycle.

The other time scale includes only average net water movements over a period of time equal to or greater than one tidal cycle. Since intertidal velocities are excluded, their affect on the concentration distribution is considered to be represented by the dispersion coefficient, D. In these models, concentrations in the channel can be calculated only at the time of slack water.

In the following literature review, methods for solving Equation 1 have been divided into three categories: analytical, numerical, and others. Both of the above mentioned time scales can be utilized by these methods.

Analytical Methods

Analytical solutions to Equation 1 can be separated into three general categories, according to the assumptions applied to the

parameters, A (area), U (velocity) and D (dispersion).

The first category includes solutions based on the assumption that equilibrium conditions exist in the estuary and that all parameters are constant with time and distance (Asano, 1967; Bain, 1968). A modified version of Equation 1 was solved with steady-state dissolved oxygen (DO) relationships in the Delaware River (O'Connor, 1960) and relatively close agreement was obtained between model predictions and observed yearly slack water concentrations. However, this type of model is often of limited value because only long term average concentrations are involved and most practical applications require knowledge about short term critical concentrations.

The second category of analytical solutions are those which hold U and D constant and allow A to vary as a simple algebraic function of X. Solutions of this type were applied to the Delaware, Upper East, and James Rivers (O'Connor, 1965) where U was set equal to the average fresh water flow over the study period. A more recent study by the same author (O'Connor, St. John, and Di Toro; 1968) utilizes similar analytic techniques. However, in this case the channel is divided into segments, the analytical solution applied to each segment, and the resulting system of simultaneous equations solved by matrix algebra. This type of model is limited to the extent that only slack water concentrations are considered and velocity fluctuations due to the tide are ignored.

The third category of analytical solutions to Equation 1 is based on the assumptions that D and A are constant and that U varies as a sinusoidal function of time. Holly (1969) used this approach for the investigation of slack water buildup associated with unsteady, uniform flow. In these studies the pollution injection rate was varied as a simple algebraic function of time. The major limiting factor of this approach is that the cross section area of the channel is considered uniform throughout the length of the estuary.

Numerical Methods

Due to the irregular geometry and unsteady flows in estuaries, Equation 1 defies analytical solution for most practical applications. Therefore, numerical methods have been utilized in order to obtain solutions with greater freedom in parameter variation. Several basic approaches to general finite-difference modeling are presented by Dresnack and Dobbins (1968) and Thomann (1963).

An implicit central-difference scheme was applied to Equation 1 for studies of the Potomac River Estuary (Harleman, Lee and Hall, 1968). The stream channel was divided into equal-length segments and average cross section areas (A) were estimated for each segment. Velocity (U) was represented as a sinusoidal function of time, the dispersion coefficient was given as a linear function of velocity, and the injection rate was a combination of continuous and slug injections.

Computer output was characterized by instability. Predicted results only vaguely resembled observed data.

In studies of the Delaware Estuary (Pence, Jeglic and Thomann, 1968), Equation 1 was combined with an oxygen balance equation and expressed as a differential-difference equation. These equations are solved numerically by fourth-order Runge-Kutta methods. Stream velocities are based on fresh water flow without consideration of tidal fluctuations. An attempt was made to incorporate the effect of tides by introducing an "advection coefficient (ξ)" into the finite difference portion of the equation. When ξ is changed from 1.0 to 5.0 the difference scheme changes from the backward to the central difference equation. Hence, the lower the value of ξ, the more dependent the concentration in a particular segment becomes on downstream concentrations. Application indicated close agreement between model and prototype for long term average DO concentrations.

Dornhelm and Woolhiser (1968) combine Equation 1 with the continuity and momentum equations for unsteady free-surface flow. The system of equations is solved by an implicit difference scheme. Instability and long periods of computer time are found to be the major disadvantages of this method.

Application of Equation 1 to a two-dimensional estuary was attempted by Orlob (1967). A square grid was superimposed on the estuary and each line segment was considered to be a one-dimensional

channel. Tidal velocities in the channels were calculated by a separate computer model. The pollution distribution was simulated by representing Equation 1 in explicit finite-difference form and applying it to each channel. Two types of numerical errors were discovered in the model; oscillations and spreading of the distribution. A sensitivity analysis comparing the central difference and quarter-point difference schemes indicated that in general when one error was reduced the other was increased.

Because of the errors introduced when Equation 1 is represented by numerical methods, some investigators have applied numerical techniques directly to the stream channel using Equation 1 only as a guide. The channel has been conceived as a series of cells each containing a known volume and uniform concentration during finite time increments (Bella and Dobbins, 1968). Convection and dispersion are simulated by average transport of material across cell boundaries and decay by reduction of cell concentrations during each time increment. A multi-step procedure is used so that the effects of each term can be determined independently. Numerical errors can be readily recognized by this procedure and a method for correction is presented. These methods are used as the basis for the mathematical model in this thesis and are explained in detail in the next chapter.

A Lagrangian concept has been developed for predicting pollution dispersion in Bolinas Lagoon, California (Fisher, 1969). The

embayment was segmented into a two-dimensional pattern; although flow with-in each segment is considered to be one-dimensional. Each time increment includes a convection step, a dispersion step, and a decay step. Convection is simulated by slugs of water moving at this average water velocity over each finite time increment. Numerical errors associated with the convection step are greatly reduced. Dispersion is an emperical relationship based on the concentration gradient.

Other Methods

Leeds and Bybee (1967) have developed a solution to Equation 1 by using digital computer programs designed to solve electrical network problems. Equation 1 is approximated by a set of ordinary differential equations obtained by replacing the differentiation with respect to the space variable with finite-differences. Stream velocities are based on fresh water flow without consideration of tidal fluctuations. Effects of mixing due to tidal action were assumed to be included in an "eddy diffusivity coefficient". Significant errors are inherent in this method, especially for the simulation of a continuous outfall (Bella, 1968).

A statistical time-series analysis was applied to concentrations in the Delaware Estuary (Thompson, 1967). Analytical techniques such as Fourier and power spectrum computations are used to

calculate DO with average daily water temperatures. The greatest amount of variance is accounted for by the annual harmonic. Frequencies at the low end of the spectrum are analyzed in detail in order to obtain a "first estimate" of the expected short term DO distribution around a mean value. Given this variance, an administrator could decide on the basis of water-use goals whether a particular mean DO concentration is sufficient in view of occasional fluctuations to critical values.

A similar type analysis was applied to Charleston Harbor (Wastler and Walter, 1968). In this case the objective was to determine effects of reduced fresh water inflow on water quality. Chloride intrusion was correlated with fresh water inflow by power spectrum analysis and a significant relationship was shown to exist between the two variables.

A stochastic model has been devided to describe the probabilistic distribution of the biochemical oxygen demand (BOD) and DO concentrations (Thayer, 1967). The model is based on the assumptions that all parameters are constant and that the system has reached steady-state conditions. Although the model is inadequate for direct application to most practical estuary problems, it does present one interesting result in that variance in DO concentration is highest when the average DO concentration is low. In other words, the greatest amount of uncertainty exists at critical concentrations.

GENERAL MODEL

General Structure

The main computer program is based on the finite-difference method developed by Bella and Dobbins (1968). The stream channel is divided into equal length segments (Δx) and the content of each segment is analyzed during finite time increments (ΔT). In this model, ΔT is less than a tidal cycle. Segments are labeled beginning with segment one at the fresh water end of the channel as shown in Figure 1, where N = segment number on the main channel and n = interface number. The program is versatile in that irregular estuary configurations can be simulated by appropriate arrangement of the segments. Tributaries can be attached to the main channel as shown in Figure 1 where K_n are segment numbers of the tributary intersecting the main channel at segment N. Mud flats can be simulated by a series of adjacent short tributaries where material is transferred across all four interfaces of each interior segment. A two-dimensional effect can be achieved by superimposing two or more channels.

The program is written in Fortran IV for use on the CDC 3300 computer at Oregon State University. Figure 2 is a flow diagram of the main program. Four types of input data are required:

1. Finite-difference grid parameters Δx and ΔT. The amount of numerical error introduced by the finite-difference scheme

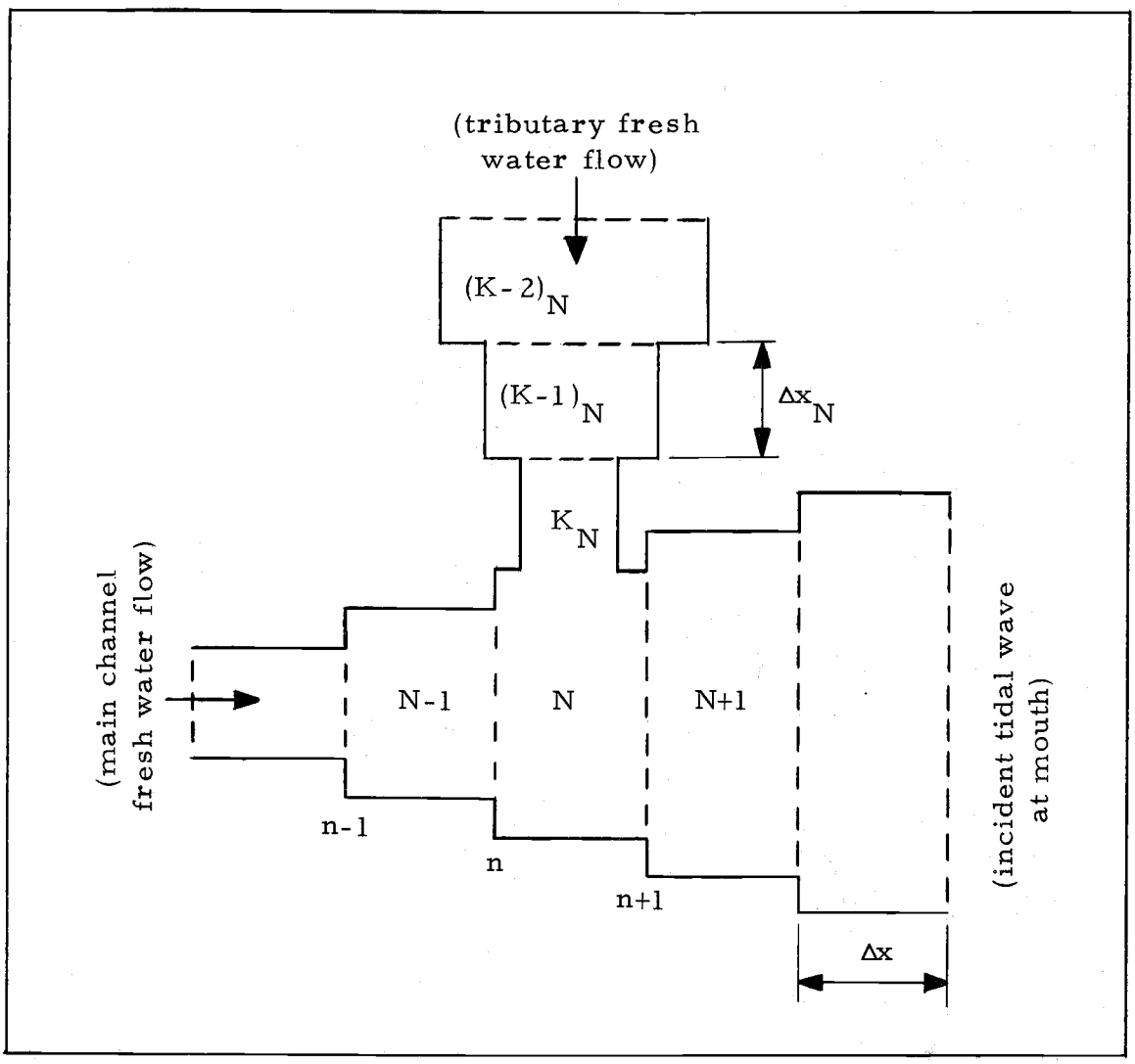

Figure 1. Representation of stream channel including a tributary.

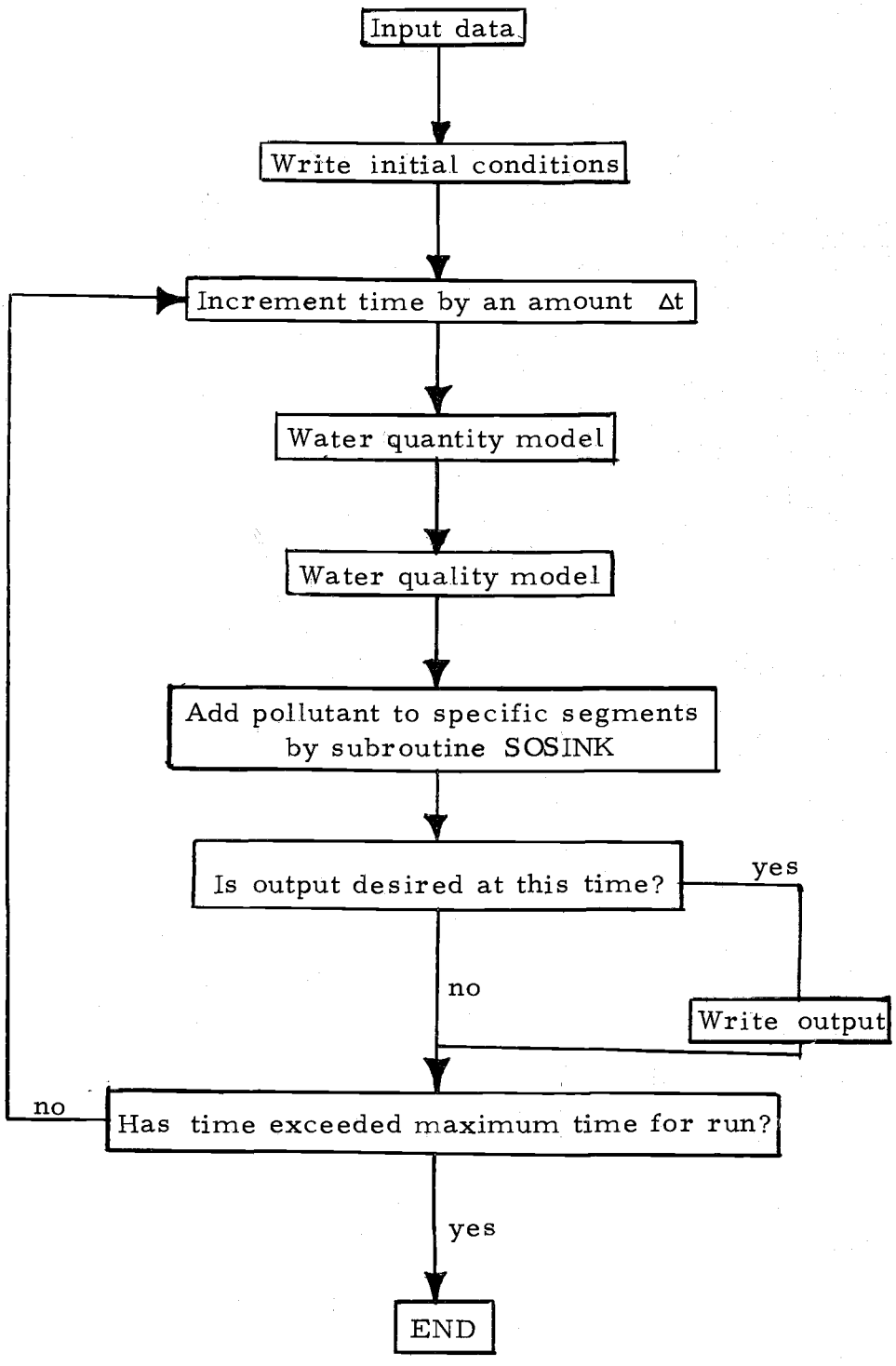

Figure 2. Flow chart for the main computer program.

was found to be very sensitive to these parameters. The numerical error is discussed in detail in the chapter ERROR STUDY.

2. Estuary configuration consisting of the cross section area, channel side slopes, and mean water depth at each segment and the location and configuration of each tributary.
3. Hydraulic characteristics of the main channel and each tributary. These data include magnitude of tidal wave at the mouth, speed of tidal wave propagation, channel friction, and fresh water inflow rates. The water quantity model is described in detail in the chapter WATER QUANTITY MODEL.
4. Mass transfer parameters and initial conditions. Those data include the dispersion and decay coefficients and the initial pollution concentration in each segment. Also included is the location of pollution sources and the rate of pollution injection at each source.

For each time increment, the program begins at the fresh water end of the main channel (segment number one) and calculates flows in each successive segment by means of the water quantity model. As the calculations proceed down the estuary, each segment is checked for an intersecting tributary. When tributaries are encountered, control is shifted to a subroutine which calculates tributary inflow. The main channel flow is adjusted by the amount of the tributary flow and

the program proceeds to the next segment.

After flows have been calculated in all segments, the program returns to segment one and again proceeds down the main channel calculating pollutant concentrations by means of the water quality model. When tributaries are encountered, control is shifted to a sub program which distributes the pollutant in the tributary.

When the pollution distribution has been calculated for all segments in the estuary, the program returns to segment number one and proceeds back down the main channel checking for pollution sources. When outfall locations are encountered pollution is injected by subroutine SOSINK.

Results are printed in predesignated times. Output includes the velocity, area, dispersion coefficient and concentration in each segment.

Water Quality Model

Convection, dispersion, and decay are considered to be the three factors acting on each segment during each time increment. Each factor is calculated independently of the others in a multi-step process. This approach allows analysis of the relative effects of each factor and simplifies detection and correction of numerical errors. In addition, any one factor can be modified or bypassed without major revision to the program as a whole.

Calculation of the convection of the pollutant between adjacent cells in the main channel is accomplished by simple mass balance considerations. The mass of pollutant transferred across an interface is equal to the volume of water which crossed the interface in time ΔT multiplied by the concentration in the upstream segment. In finite-difference terms the concentration in segment N at $T + \Delta T$, when flow is towards the ocean, can be represented as:

$$C_{(N, T+\Delta T)}A_{(N, T+\Delta T)}\Delta x = C_{(N, T)}A_{(N, T)}\Delta x + UA_{(n, T)}C_{(N-1, T)}\Delta T - UA_{(n+1, T)}C_{(N, T)}\Delta T \qquad (2)$$

where $C_{(N, T)}$ = concentration in segment N at time T, $A_{(N, T)}$ = average area of segment N at time T and $UA_{(n, T)}$ = average flow across interface n during period ΔT. Equation 2 is modified when flow is in the opposite direction by changing the sign on UA and changing the subscripts on C from N-1 to N and from N to N+1 in the last two terms. Numerical errors are introduced by this method of simulating convection. The properties of these errors and a method for correction are presented in the chapter on numerical errors.

Dispersion describes the transfer of mass across segment interfaces caused by non-uniform cross section velocity gradients. It can be represented in explicit finite-difference form as follows (Bella

and Dobbins, 1968):

$$C_{(N, T+\Delta T)} = C_{(N, T)} + F_1[C_{(N+1, T)} - C_{(N, T)}] + F_2[C_{(N-1, T)} - C_{(N, T)}] \quad (3)$$

$$F_1 = \frac{DA_{(n+1, T)}\Delta T}{A_{(N, T)}(\Delta x)^2}$$

$$F_2 = \frac{DA_{(n, T)}\Delta T}{A_{(N, T)}(\Delta x)^2}$$

where D = a dispersion coefficient which may vary with N and T.

Decay is represented in the model by reducing $C_{(N, T)}$ by a fractional amount of the average concentration in a segment during ΔT. Written in finite-difference form:

$$C_{(N, T+\Delta T)} = C_{(N, T)} - K[(1-\theta)C_{(N, T)} + \theta C_{(N, T+\Delta T)}]\Delta T \quad (4)$$

where θ is a weighting factor for obtaining the average value. Solving Equation 4 for $C_{(N, T+\Delta T)}$ gives:

$$C_{(N, T+\Delta T)} = C_{(N, T)}\left[\frac{1-K\Delta T(1-\theta)}{1+K\Delta T\theta}\right] \quad (5)$$

When a tributary is encountered, control is shifted to a subprogram which calculates the pollution concentration in the tributary segments in a manner analogous to that used in the main channel. Mass

transfer between the last segment in the tributary and the main channel segment is accomplished by equations similar to Equations (2) and (3).

Sources and Sinks

A quantity of pollutant mass can be added or subtracted from specific segments during each time interval by means of subroutine SOSINK. The quantity of mass can be varied as a function of time in order to simulate realistic pollutant outfall or sink characteristics. The concentration in the segment is adjusted according to the total pollutant mass and the volume of water currently in the segment.

Because concentrations are considered to be uniform in each channel segment, a particular pollutant source or sink cannot be located with greater accuracy than the length of Δx. Outfalls located at any point within a segment will, for example, have the same affect on model results.

If subroutine SOSINK is included in the program before the water quality model, it is possible for unrealistic distributions to appear in the output. For example, in the case of a continuous pollution source and relatively high stream velocities, the printout indicates that maximum concentrations occur in the first segment downstream from the simulated outfall instead of in the segment containing the outfall. Therefore, this subroutine has been included after the water quality model.

WATER QUANTITY MODEL

Method

The most simple method for estimating stream velocities is to assume uniform flow throughout the estuary and apply a sinusoidal velocity at the mouth (Bella and Dobbins, 1968; Harleman, 1968; Holley, 1969). A more realistic method is to determine water surface elevations as a function of distance and time and calculate flows from known characteristics of the channel. This can be accomplished by solving the continuity and momentum equation for unsteady flow (Dornhelm and Woolhiser, 1968). Although this method is accurate, a great amount of computer time is required. A more efficient method has been to use changes in water surface elevations to calculate average flows over small time intervals, i. e., (average flow out of segment) = (average flow in) - (change in volume), (Fisher, 1969). This method has been adopted for the present study and can be represented in finite-difference terms as follows for flow in the direction shown in Figure 1:

$$UA_{(n,\,T)} = UA_{(n-1,\,T)} + \left[A_{(N,\,T-1)} - A_{(N,\,T)}\right] \frac{\Delta x}{\Delta T} \qquad (6)$$

By using this approach, the problem is reduced to one of finding an efficient means for predicting water surface elevations(H).

Fisher (1969), in studies of Bolinas Lagoon, California, used observed values of H over a few tidal cycles. The use of tabulated values becomes awkward for long periods of analysis. Dorlhelm and Wollhiser (1968) predict H by propagating a sine shaped tidal wave up the estuary. Tidal actions in most real estuaries do not conform to this simple representation however.

Frequently a reflected sine wave can be used to predict tidal heights along an estuary (Ippen, 1966). Consider the channel profile of length L shown in Figure 3. An imposed wave is assumed to travel up the estuary from the mouth. A hypothetical boundary exists at the end of the estuary which reflects a portion of the incident wave. The water surface at a point x feet from the boundary can be predicted by superimposing the height of the reflected wave onto the incident wave. The effects of friction can be approximated by assuming an exponential reduction in wave height with distance. Mathematically, the tidal height can be represented as (Glenne, 1969):

$$H = H_0 + a\left[e^{\mu x}\cos(\delta T + kx) + \beta e^{-\mu x}\cos(\delta T - kx)\right] \qquad (7)$$

Where H_0 = average water surface elevation, a = amplitude of incident wave, μ = constant representing channel friction, δ = wave frequency, k = portion of a tidal cycle required for the wave to travel one unit of estuary length, and β = fraction of wave reflected. For short tributaries the water surface elevation can be assumed equal to that

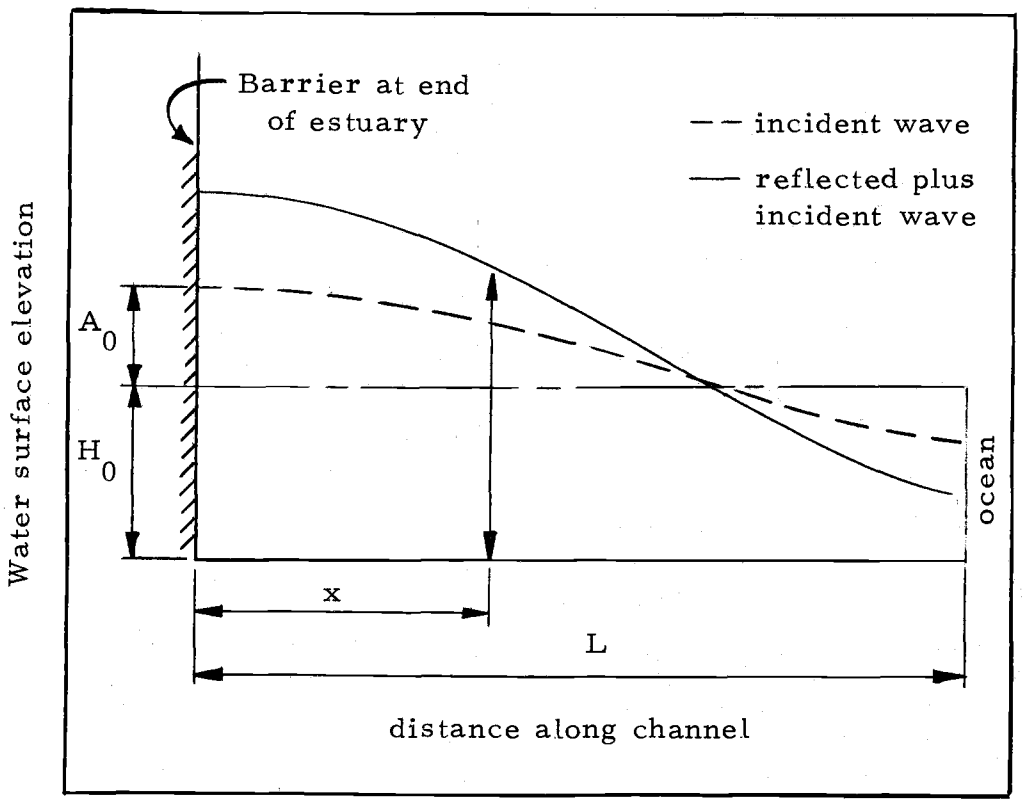

Figure 3. Reflected tidal wave.

in the main channel at the point of intersection. For long tributaries, program control is shifted to a subprogram which propagates the wave up the tributary channel in accordance with Equation 7 where a = amplitude of incident wave at the mouth of the tributary.

The solution of Equation 7 for every channel and tributary segment during each time increment would be very time consuming. Therefore a method of approximating Equation 7 was adopted. Figure 4 shows the flow chart for the subprogram used to calculate water surface elevations and cross section areas. The incident wave at the mouth of the estuary is represented for one and a quarter tidal periods by a series of chords as shown in Figure 5. This method of describing the wave allows complete freedom for selecting any shape wave at the mouth of the estuary, i. e., it is not limited to a cosine function. The amount of error introduced by representing a smooth curve with a series of chords is a function of the number of increments into which the tidal cycle is divided. The error in representing a cosine curve by this method is shown in Figure 6 where ι is the maximum difference between any chord and the true curve based on an amplitude of one.

For any particular time at the mouth of the estuary, T, the ordinate of the imposed wave at any point, x, in the estuary can be calculated by determining the time required for the wave to move up the channel to that point. This is the lag time and is represented by

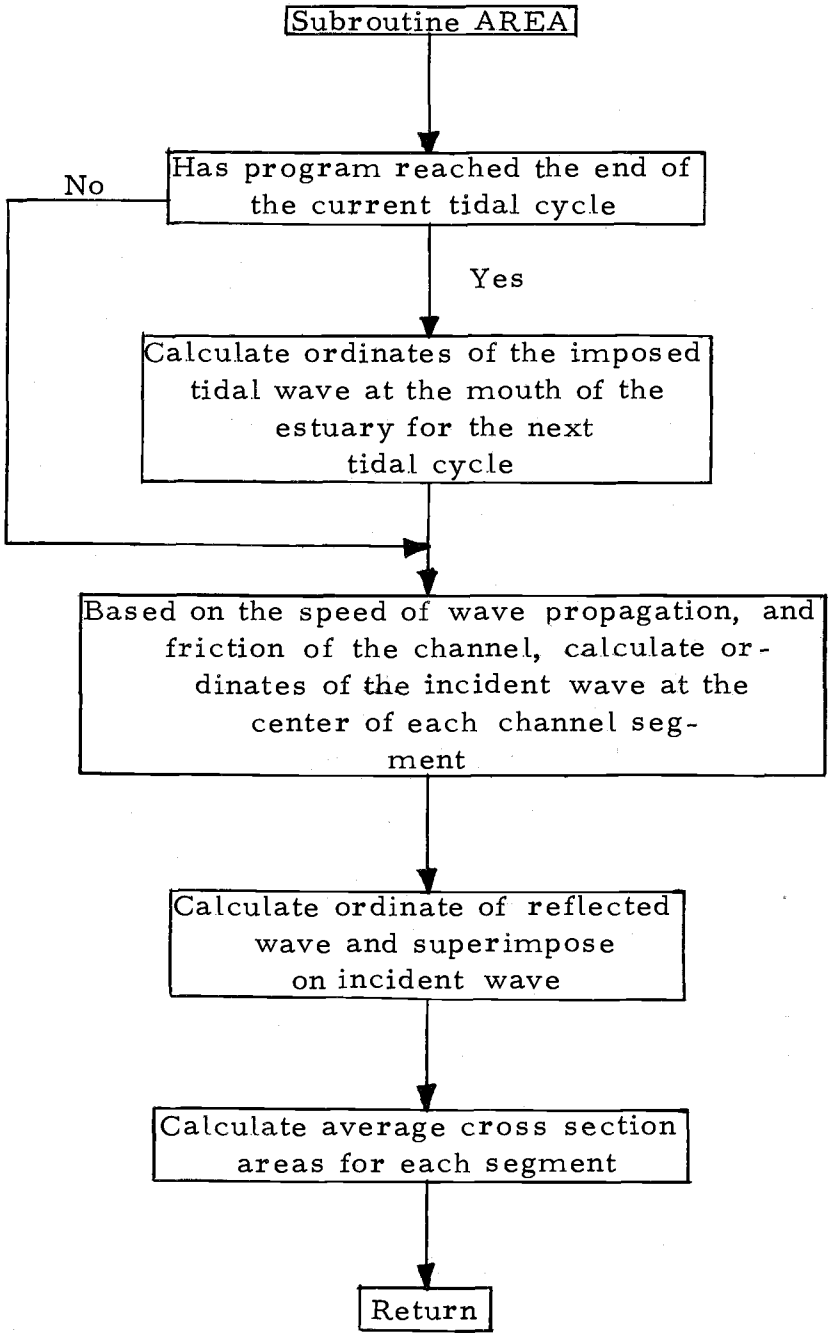

Figure 4. Flow chart for subroutine AREA.

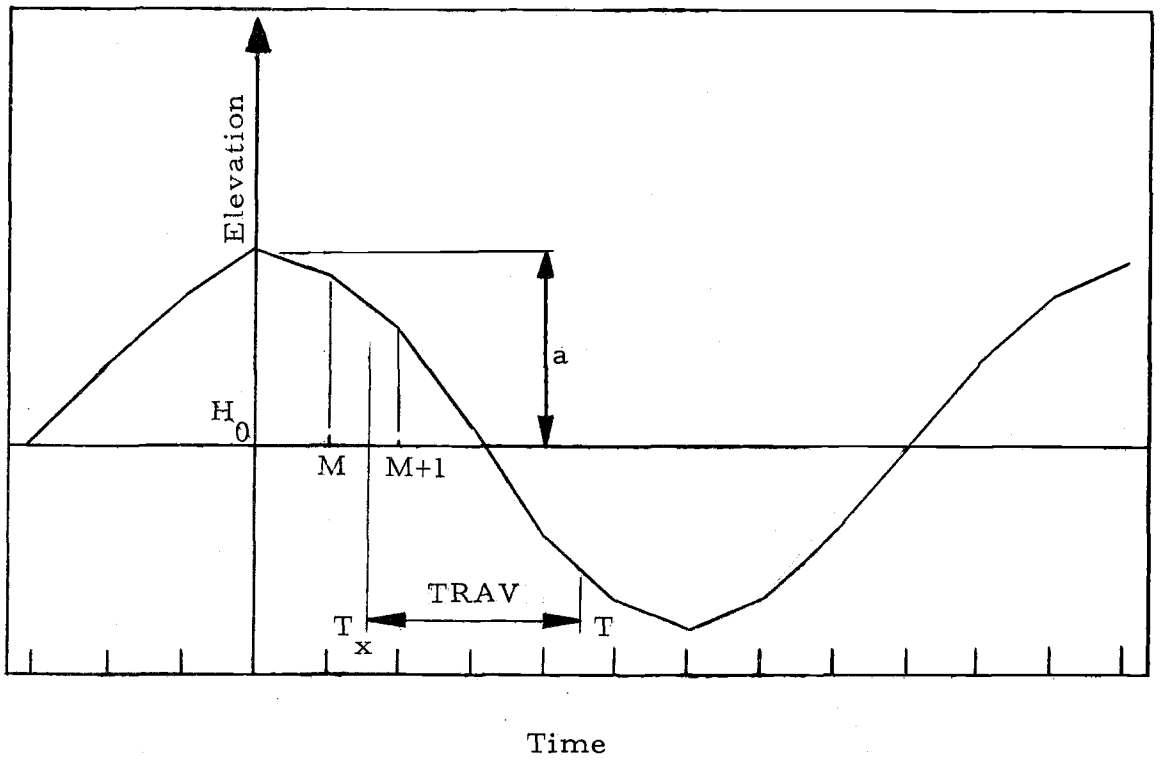

Figure 5. Tidal wave representation at the mouth of an estuary.

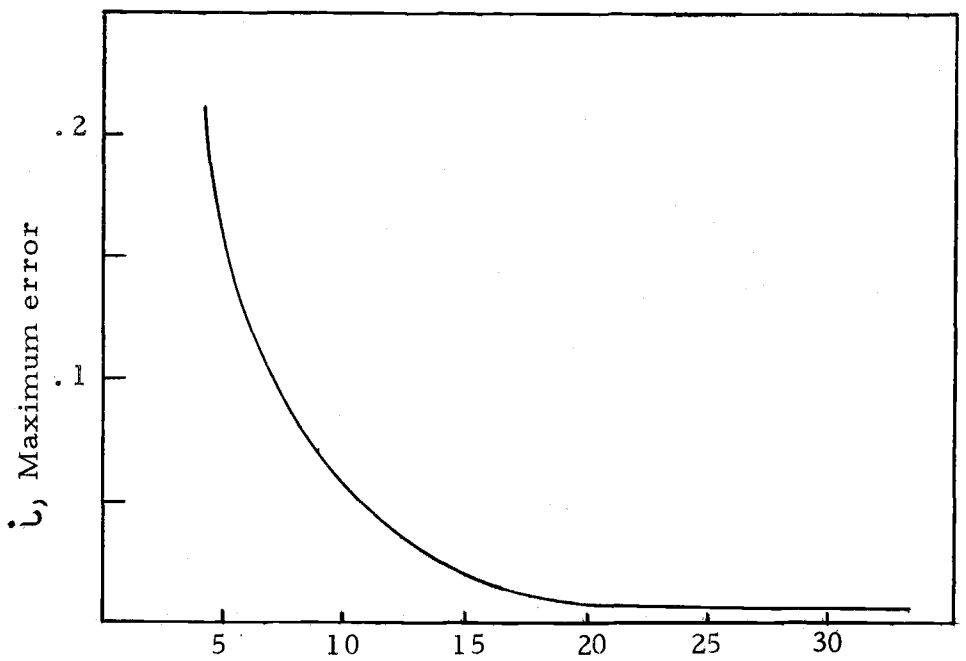

Figure 6. Error introduced by linear interpolation.

TRAV on Figure 5. For this study, the time lag was expressed as :

$$TRAV = c(L-x)$$

where c is wave celerity, x is the distance from the fresh water end, and L is the length of the estuary. More accuracy could possibly be achieved by allowing c to vary as a function of depth; however, at the sacrifice of computer time. Once T_x is located (Figure 5), the elevation is obtained by interpolating between points M and M +1.

The ordinate of the reflected wave is obtained in a similar manner. A portion of the incident wave is assumed to bounce off the boundary at the end of the estuary and travel back towards the mouth at the same celerity. The total lag time for the wave to travel from the mouth back to point x can be calculated by:

$$TRAV = c(L+x)$$

Friction is incorporated in the model by reducing the ordinates by an exponential function of the distance traveled by the wave, i. e., $e^{-\mu(L-x)}$ for the incident wave and $e^{-\mu(L+x)}$ for the reflected wave. The water surface elevation is then obtained by superimposing the ordinates of the incident and reflected waves. Friction need not be represented by an exponential function; however, it was selected so that existing methods (Ippen, 1966) could be used to estimate the parameters μ and k. It may not be the most realistic representation,

however, because the major frictional influence is exerted near the mouth of the estuary and the frictional effect decreases with distance up the estuary. Conversely, in some real estuaries the effect of friction would probably be least near the mouth and increase with distance up the estuary.

Cross section areas are calculated as a function of the water surface elevation and side slopes of the channel at each segment.

Boundary Conditions

In order to calculate flows by means of Equation 6 it is necessary to know the flow across the interface of segment one at the upper end of the estuary and in every tributary. For a completely reflected wave all of the tidal induced flow is reflected and, therefore, the flow across the first interface is equal to the fresh water inflow. Physically this can be visualized as a waterfall forming a complete barrier at the end of the estuary. However, when the upstream boundary reflects only a fraction, β, of the incident wave amplitude, a certain amount of flow will be induced at segment one due to tidal action beyond the boundary. When this flow is neglected, significant errors may be introduced for values of β less than one.

The tidal induced flows at the boundary can be calculated by extending the hydraulic model beyond the boundary a distance necessary for the unreflected portion of the wave to become significantly

attenuated by friction. For progressive waves with low friction this method may require excessive computer time. One approach to reduce computer time and still approximate flows across the first interface would be to increase the friction coefficient beyond the boundary. Errors introduced by this approximation would have to be investigated for each individual case.

If the reflected wave is not completely attenuated when it reaches the mouth of the estuary, the calculated water surface elevation will not coincide with the incident wave and a discontinuity will occur at the ocean boundary. Ippen (1966) avoids the problem by applying the incident wave at the end of the estuary instead of the mouth. However, tidal fluctuations are generally not recorded at the upper end of an estuary, and this approach is not always practical.

If there is sufficient friction in the channel, or if β is low, the discontinuity will be neglible. When a substantial discontinuity does exist at the ocean boundary, a driving wave must be found such that superposition of the reflected wave will result in water surface elevations which agree with observed data. Finding a driving wave is difficult, but it can be done by trial and error for short runs.

Testing

An analytical solution for a uniform rectangular channel was developed and compared with computer output in order to determine how accurately the program predicted flows.

In a rectangular channel with constant width, B, flow can be represented by the following equation:

$$d(UA) = B \frac{\partial H}{\partial T} dx \tag{8}$$

Substituting Equation 7 into Equation 8:

$$UA = B\delta a \int_0^x [e^{\mu x}\sin(\delta T+kx) + \beta e^{-\mu x}\sin(\delta T-kx)]\, dx \tag{9}$$

Intergrating each term in Equation 9 by parts twice and combining terms leads to:

$$UA = F_3 e^{\mu x}[\cos(\delta T+kx+\alpha) - \beta F_3 e^{-\mu x} \frac{k^2+\mu^2}{k^2+\beta\mu^2}[\cos(\delta T-kx+\alpha)] \tag{10}$$

$$F_3 = \frac{Ba\delta}{\sqrt{k^2+\mu^2}}$$

α = arc tan μ/k

When $\beta = 1$, the wave is completely reflected and Equation 10 reduces to the form developed for a standing wave (Ippen, 1966).

Equation 10 predicts that maximum flow will lag slack water by approximately ninety degrees for a completely reflected tidal wave.

As β decreases, the lag time between high water and maximum flow decreases. Maximum flow approximately coincides with high water for a progressive tidal wave, when $\beta = 0$.

The percentage error between computer results and the analytical solution is shown in Table 1 for seven runs. The amplitude of the imposed wave was 3.5 feet at the mouth of the estuary and the wave was considered to travel up the estuary at a constant speed of 25 feet per second (k=0.04). The length of the estuary was 25 miles. Values were recorded at two times during the tidal cycle in order to compare errors associated with both high and moderate flows. Tidal heights predicted by the program were within 1% of those calculated by Equation 7 for all runs. High flows for runs number one and number two were unrealistic and, therefore, not included in Table 1.

Runs number one and three and runs number two and five are identical pairs with the exception of the friction coefficient, μ. Comparison of these runs indicates that the introduction of friction increases the error associated with the finite difference scheme. Comparison of runs number three and four and runs number five and six indicates that error is not affected by reducing Δx when ΔT is relatively large and is only slightly affected by reducing Δx when ΔT is small. The error is, however, significantly reduced by decreasing ΔT from 1/4 hours to 1/6 hours as shown in runs number four and five. In general, the error was reduced more by decreasing the time

Table 1. Computer run parameters and percent error associated with each run.

Run #		1	2	3		4		5		6		7	
Δx (miles)		0.50	0.25	.50		.25		.25		.10		.10	
ΔT (hr)		1/4	1/6	1/4		1/4		1/6		1/6		1/6	
μ (miles)$^{-1}$		0	0	0.092		0.092		0.092		0.092		0.092	
β		1	1	1		1		1		1		.75	
Percent error at two fractions of a tidal cycle													
		1/2	1/2	1/4	1/2	1/4	1/2	1/4	1/2	1/4	1/2	1/4	1/2
Distance from boundary	5.25	1.1	1.7	1.1	10.9	4.1	8.5	1.9	2.7	0.0	1.1	0.6	2.0
	10.25	3.7	1.5	4.5	7.9	5.8	6.2	1.5	2.2	0.7	1.2	2.5	6.0
	15.25	4.7	1.4	8.0	6.5	9.4	5.1	2.0	1.8	1.5	1.0	3.6	8.9
	20.25	5.1	0.9	12.4	5.6	13.0	4.3	1.2	1.6	1.0	0.8	5.3	10.7
	24.75	5.3	0.6	17.7	4.6	18.2	3.4	1.1	1.6	1.1	0.9	8.0	11.5

increment than by decreasing the segment length. Run number five appears to be about an optimum balance between computer time and numerical error.

For run number seven the barrier at the fresh water end of the estuary was considered to be only partially reflecting, $\beta = 0.75$. The influence on flow of tidal conditions above the barrier was neglected and the resulting error was significant as can be observed by comparing run seven with run six.

ERROR STUDY

Introduction

A basic component of most mathematical models of aquatic ecosystems involves the movement of materials carried by the water (convection). The differential equation describing convection due to uniform flow in a channel of constant cross-sectional area is given by

$$\frac{\partial C}{\partial T} = -U\frac{\partial C}{\partial x} \qquad (11)$$

in which C is the water carried material (tracer, pollutant, etc.) concentration, T is time, U is the water velocity and x is the longitudinal distance.

Finite-difference methods commonly used in developing numerical models most often poorly describe this very basic convection process. Finite-difference convection errors are often subtle, affecting the results in a manner not intended by the investigator yet often escaping notice and thus possibly contributing to the misinterpretation of model results.

It is the purpose of this chapter to go back to the simplicity of pure convection and investigate the errors associated with several commonly used finite-difference convection approximations. It is intended that this investigation into this most basic process will contribute to the ability of and confidence in the more complex finite-difference

models of aquatic ecosystems that are presently being developed. For simplicity, the investigation will consider only one-dimensional convection (downstream movement) for uniform flow in a water channel of constant cross-sectional area.

Errors of different finite-difference approximations of convection have been recognized by previous investigators.

During studies for the Sacramento-San Joaquin Delta (Orlob, Shubinski and Feigner, 1967) the numerical convection error was described as "numerical mixing" with the magnitude related to the ratio

$$\alpha = \frac{U\Delta T}{\Delta x} \tag{12}$$

In these studies, the numerical mixing was so high that actual dispersion was not separately included within the model.

During studies on the Potomac River Estuary (Harleman, Lee and Hall, 1968) large numerical errors were generated by shock loadings. These errors were minimized by modifying computer input injection rates to more evenly distribute the loads.

The numerical spreading errors associated with the backward or upstream difference method have been quantified by a pseudo dispersion coefficient (Bella and Dobbins, 1968) given by

$$D_p = \frac{U}{2}[\Delta x - U\Delta T) \tag{13}$$

for a stream of constant cross section and uniform flow.

A similar dispersion coefficient describing the spreading associated with the central difference equation has been presented (Prych and Chidley, 1969) as

$$D = \frac{U^2 \Delta T}{2} \tag{14}$$

Numerical Convection Model

Finite-difference representation of smooth distributions can be visualized as a series of completely mixed cells as shown in Figure 7. Numerical convection can be visualized as the transfer of material over successive time intervals from cell to cell in the downstream direction. The following study of numerical convection will be limited to finite-difference models in which the concentration change within a cell due to convection over a finite time interval, ΔT, is determined by the concentrations within the cell and within adjacent cells at the beginning of the time interval. A general finite-difference equation of such convection is given by

$$C_{(N, T+\Delta T)} = C_{(N, T)} + F[(1-\gamma)C_{(N-1, T)} + \gamma C_{(N, T)}] - F[(1-\gamma)C_{(N, T)} + \gamma C_{(N+1, T)}] \tag{15}$$

where $F = \frac{U \Delta T}{\Delta x}$ and γ is a proportionality factor used to establish flux between cells. In Equation 15,

$\gamma = 0.00$, reduces Equation 15 to the upstream difference

equation;

$\gamma = 0.25$, reduces Equation 15 to the quarter point difference equation;

$\gamma = 0.50$, reduces Equation 15 to the central difference equation, and;

$\gamma = 1.00$, reduces Equation 15 to the downstream difference equation.

F can be physically interpreted as the fraction of a cell length (Δx) traveled by a particle of water during the time interval ΔT. Figure 8 illustrates the nature of Equation 15 by showing the convection of a slug distribution over one time interval, ΔT.

Numerical Convection Errors

Finite-difference convection errors were investigated by numerically convecting a slug load represented by a uniform concentration of 100 within a single cell. If no errors were present, the centroid of the distribution moved downstream at the chosen velocity and the concentration distribution remained unchanged.

Figure 9a shows the distribution resulting from a typical run in which the parameters $U = 18$ mi/day; $\Delta x = 0.05$ mi, $\Delta T = 1/96$ days and $\gamma = 0.25$ were used. Boundaries were located at a distance sufficiently large from the distribution center so as to have very little effect on the distribution. Comparing these results to the pure

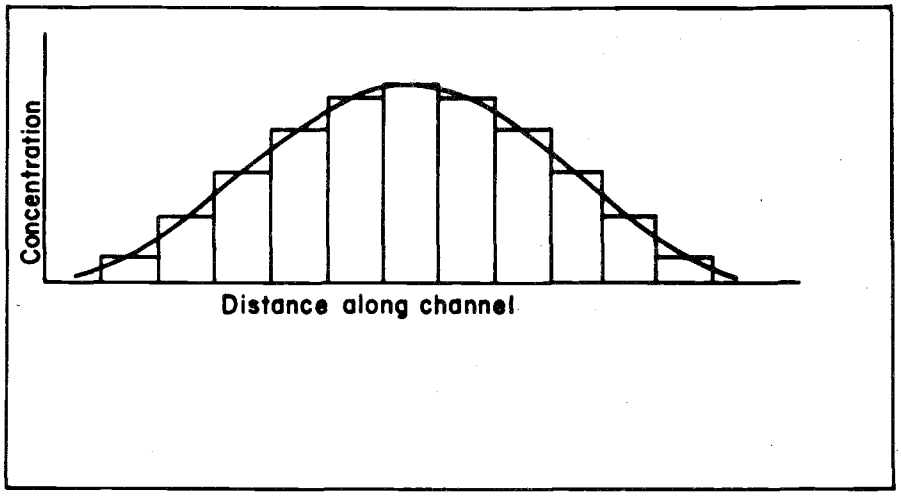

Figure 7. Finite difference approximation of a continuous function.

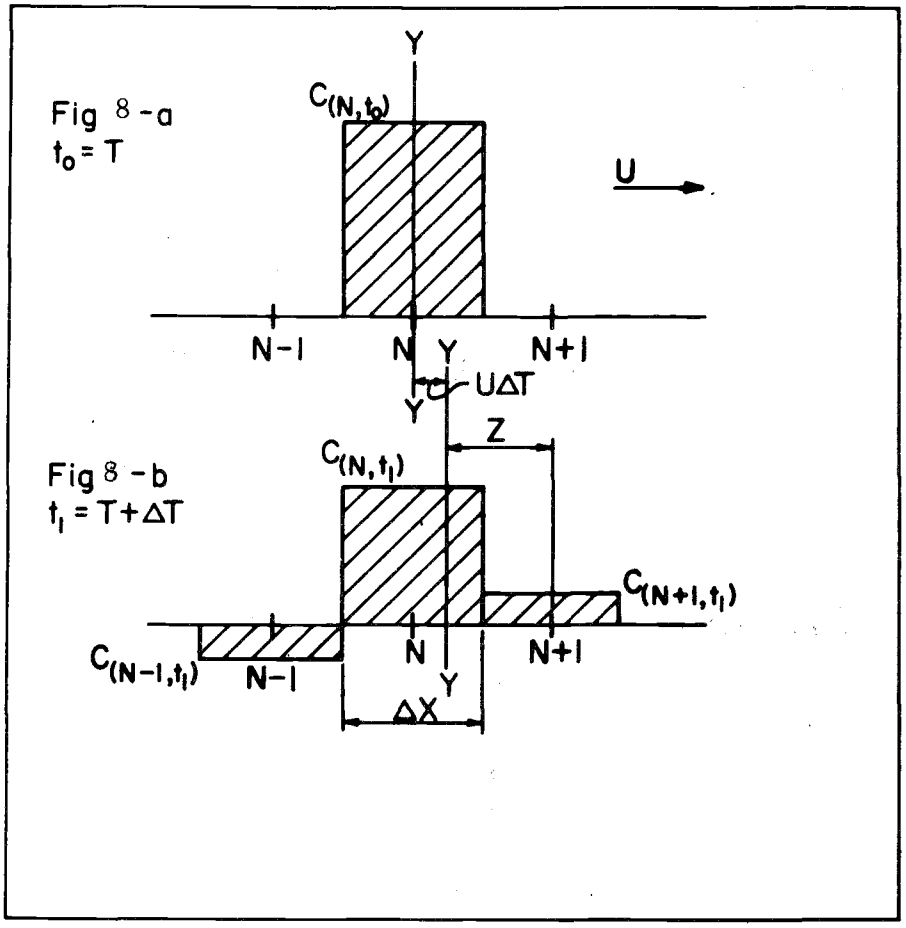

Figure 8. Convection of a slug load, illustrating the central difference approximation.

translation of the initial slug reveals the nature of the errors typical of finite-difference convection models. The nature of these errors will be classified into three categories.

The first category of errors is called oscillation errors and can be noticed by the left side (upstream) of the numerical distribution shown in Figure 9a. The variation between positive and negative concentrations over a short distance can either decrease to small magnitudes or can increase to extremely large values as the numerical convection calculations proceed. These oscillations result from the numerical removal of more material from a cell over a time interval than is present within that cell at the beginning of that time interval.

The oscillations associated with different convection models will be defined by the magnitude of the largest calculated negative concentration present at a given time. In Figure 9a, the oscillation error is given as 3.4.

The second category of errors is seen by the skewness of the numerical distribution shown in Figure 9a. This error will be defined by the magnitude of the skewness as computed by:

$$\text{(Normalized third moment about centroid)}/(\text{Variance})^{3/2} \tag{16}$$

The computed distribution shown in Figure 9a has a skewness of 2.64.

The third category of errors is characterized by the spreading of the distribution as shown in Figure 9a. This spreading is

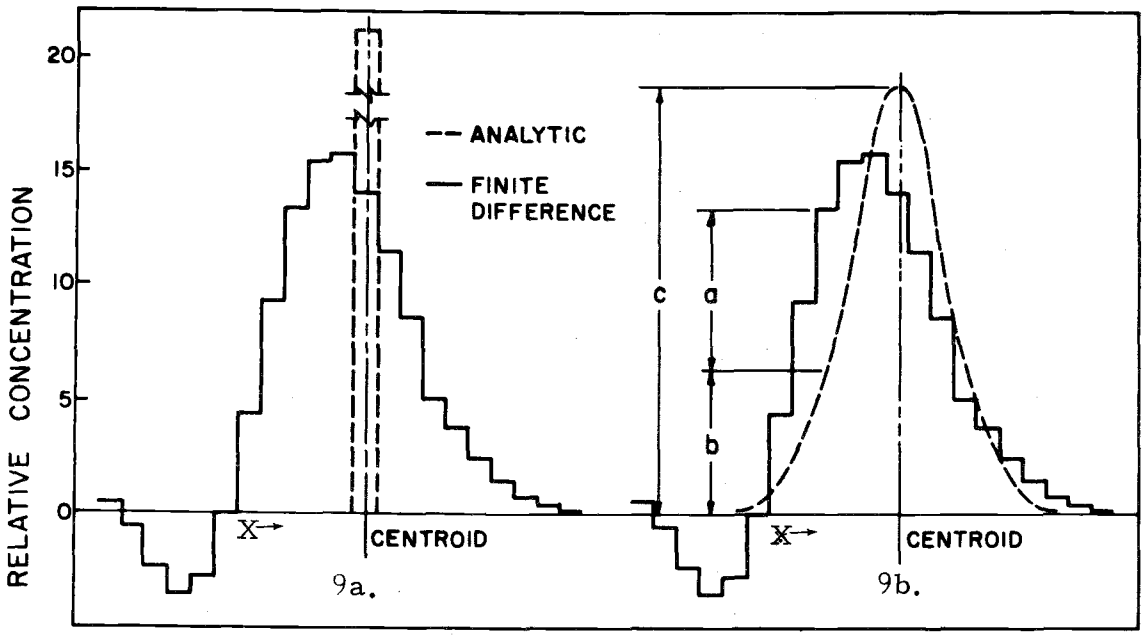

Figure 9. Distortions introduced by the convection term.

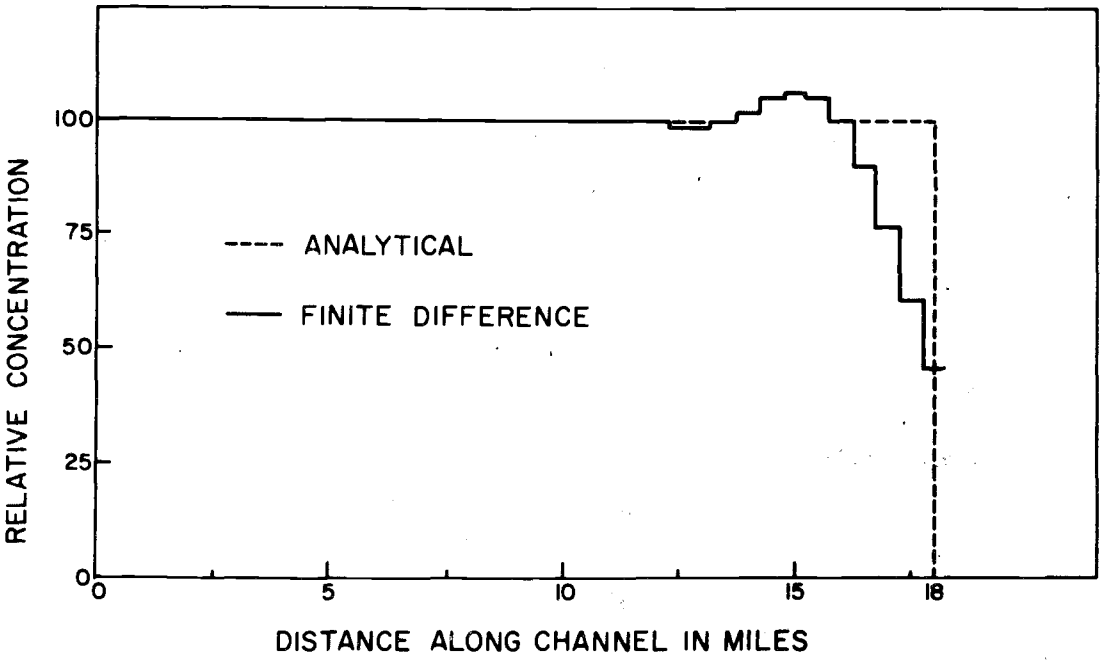

Figure 10. Superposition of slug loads.

expressed by a pseudo dispersion coefficient given by:

$$D_p = \frac{1}{2}(\text{rate change in variance}) = \frac{1}{2}\frac{\Delta\delta^2}{\Delta T} \qquad (17)$$

where

$$\text{Variance} = \delta^2 = \frac{\int_{-\infty}^{\infty} \xi^2 C d\xi}{\int_{-\infty}^{\infty} C d\xi} \qquad (18)$$

and ξ = the distance from the centroid to C (Fisher, 1966). When the distribution consists of adjacent rectangles as in Figure 8, variance can be expressed as:

$$\delta^2 = \frac{\sum_{i=1}^{M} [Z_i^2 \Delta x C_i + \Delta x^3 C_i/12]}{\sum_{i=1}^{M} \Delta x C_i} \qquad (19)$$

where Z_i = the distance from the centroid of the entire distribution to the centroid of the rectangular area $\Delta x C_i$.

In an actual stream, pollutants and tracers are spread along the length of the stream by velocity gradients and turbulent water motions. The magnitude of this spreading is often included in mathematical stream models through a longitudinal dispersion coefficient. For the conditions of a constant dispersion coefficient and a constant cross-sectional area, dispersion is mathematically described by:

$$\frac{\partial C}{\partial T} = D \frac{\partial^2 C}{\partial x^2} \qquad (20)$$

in which the dispersion coefficient D can be expressed and measured by Equation 17. Thus, the magnitude of the spreading error in numerical convection models is quantified in terms of an often used physical coefficient. This greatly assists an investigator in determining how much the error affects the results. The pseudo dispersion coefficient describing the numerical spreading shown in Figure 9a is 0.5625 square miles per day.

The errors shown in Figure 9a can often be masked when smooth distributions are calculated. As an example consider Figure 10 which shows the distribution for a run in which the same numerical model and parameters shown in Figure 9a were used. A slug load, however, was not convected but instead, the upstream boundary was held at a constant value and initial conditions of zero concentration throughout the length were assumed. With the exception of the concentration front, the smooth portion of the numerical distribution closely agrees with the analytical results despite the fact that numerical convection of a slug load is very poorly described (Figure 9a). The smooth numerical distribution can be visualized as a series of slug distributions. In the smooth distribution the errors are superimposed and thus masked; hence, a satisfactory computation of a smooth distribution is a poor test of the accuracy of a numerical model.

Tests of numerical methods using slug loads are far more informative.

The results of a series of computer runs using slug loads and different numerical convection models are summarized in Table 2. The three categories of errors discussed above are listed in columns (7), (8) and (9).

Pure translation was simulated only in runs 1 and 8 in which the backward difference equation ($\gamma = 0.00$) was used with F equal to unity. The backward difference method displayed no oscillations and only slight skewness. However, a relatively large amount of positive dispersion was not uncommon.

Severe oscillations and negative dispersion typified results from the central difference equation ($\gamma = 0.5$) and the forward difference equation. Frequently, oscillations became larger as computations progressed.

The quarter point equation displayed a wide range of errors within all categories. Both negative and positive dispersion was obtained. Positive dispersion tends to reduce concentration gradients while negative dispersion tends to increase the gradients. As a result, runs in which negative psuedo dispersion was present experienced a growth of oscillations as computations progressed while a reduction of oscillations was found when positive pseudo dispersion was present.

An investigator might also reason that by reducing ΔT, errors are reduced, yet, an inspection of the dispersion error associated

Table 2. Convection of slug load by different numerical schemes.

Run No.	γ (1)	Δx (Miles) (2)	ΔT (Days) (3)	F (4)	Centroid (Miles) (5)	One-half Rate Change in Variance, ($Miles^2$ per day) (6)	Skewness (7)	Oscillations (8)	D_p^2 ($Miles^2$ per day) (9)
1	0.00	1.00	1/12	1.000	24	0.000	0.00	0.0	0.000
2	0.00	1.00	1/16	0.750	24	1.500	0.20	0.0	1.500
3	0.00	1.00	1/24	0.500	24	3.00	0.00	0.0	3.000
4	0.00	1.00	1/48	0.250	24	4.500	0.12	0.0	4.500
5	0.00	1.00	1/96	0.125	24	5.250	0.16	0.0	5.250
6	0.00	0.50	1/48	0.500	24	1.500	0.00	0.0	1.500
7	0.00	0.50	1/96	0.250	24	2.250	0.08	0.0	2.250
8	0.00	0.25	1/48	1.000	24	0.000	0.00	0.0	0.000
9	0.00	0.25	1/64	0.750	24	0.375	0.10	0.0	0.375
10	0.00	0.25	1/96	0.500	24	0.750	0.00	0.0	0.750
11	0.25	1.00	1/12	1.000	24	-3.000	0.87	578.2	-3.000
12	0.25	1.00	1/16	0.750	24	-1.500	1.67	73.3	-1.500
13	0.25	1.00	1/24	0.500	24	0.000	748.25	10.8	0.000
14	0.25	1.00	1/48	0.250	24	1.500	1.20	1.6	1.500
15	0.25	1.00	1/96	0.125	24	2.250	0.74	0.6	2.250
16	0.25	0.50	1/24	1.000	24	-1.500	0.62	13921.1	-1.500
17	0.25	0.50	1/32	0.750	24	-0.750	1.17	187.5	-0.750
18	0.25	0.50	1/48	0.500	24	0.000	1496.49	10.1	0.000
19	0.25	0.50	1/64	0.375	24	0.375	2.30	2.8	0.375
20	0.25	0.50	1/96	0.250	24	0.750	0.86	0.8	0.750
21	0.25	0.25	1/48	1.000	24	-0.750	0.43	*****	-0.750
22	0.25	0.25	1/64	0.750	24	-0.375	0.82	1636.0	-0.375
23	0.25	0.25	1/96	0.500	24	0.000	2992.98	8.6	0.000
24	0.50	1.00	1/12	1.000	24	-6.000	0.62	68988.1	-6.000
25	0.50	1.00	1/48	0.250	24	-1.500	1.87	264.1	-1.500
26	0.50	1.00	1/96	0.125	24	-0.750	4.97	69.1	-0.750

continued on next page

Table 2 continued.

Run No.	γ (1)	Δx (Miles) (2)	ΔT (Days) (3)	F (4)	Centroid (Miles) (5)	One-half Rate Change in Variance (Miles^2 per day) (6)	Skewness (7)	Oscillations (8)	D_p (Miles^2 per day) (9)
27	0.50	1.00	1/192	0.0625	24	-0.3750	14.34	33.7	-0.3750
28	0.50	1.00	1/348	0.03125	24	-0.1875	50±	23.0	-0.1875
29	0.50	0.50	1/24	1.000	24	-3.000	0.43	*****	-3.000
30	0.50	0.50	1/48	0.500	24	-1.500	0.63	533677.8	-1.500
31	0.50	0.50	1/96	0.250	24	-0.750	1.31	3344.1	-0.750
32	0.50	0.25	1/48	1.000	24	-1.500	0.21	*****	-1.500
33	0.50	0.25	1/96	0.500	24	-0.750		*****	-0.750
34	1.00	1.00	1/96	0.125	24	-6.750		*****	-6.750

All runs with constant velocity, U = 12 miles/day. Values were recorded at time = 2 days.

***** Value greater than 9×10^6.

with the backward difference equation (Table 2) reveals that this error increases as ΔT decreases when U and Δx are held constant. Reducing ΔT might then maximize the error rather than minimize it.

The results shown in Table 2 indicate that one or two types of errors can often be reduced with a resulting increase in the remaining errors. Thus, run 13 has no dispersion error yet its skewness and oscillations are high (see Figure 11). Run 15, using the same value of γ, has a higher pseudo dispersion and the skewness and oscillation errors are reduced (see Figure 11). Run 17 has low dispersion and skewness errors yet the oscillations are quite high (see Figure 12). In these examples, the relative magnitudes of the different errors have changed yet none of the results satisfactorily describe pure convection.

This apparent trade off of errors does suggest a method of error control. If an estimate of the dispersion error is available, an investigator might select a method which reduces the skewness and oscillation errors to minimum levels and in the process increases the dispersion error. The estimate of the dispersion error might then provide a reasonable estimate of the entire numerical convection error. The magnitude of the error would then be defined and correction of the error might then be made.

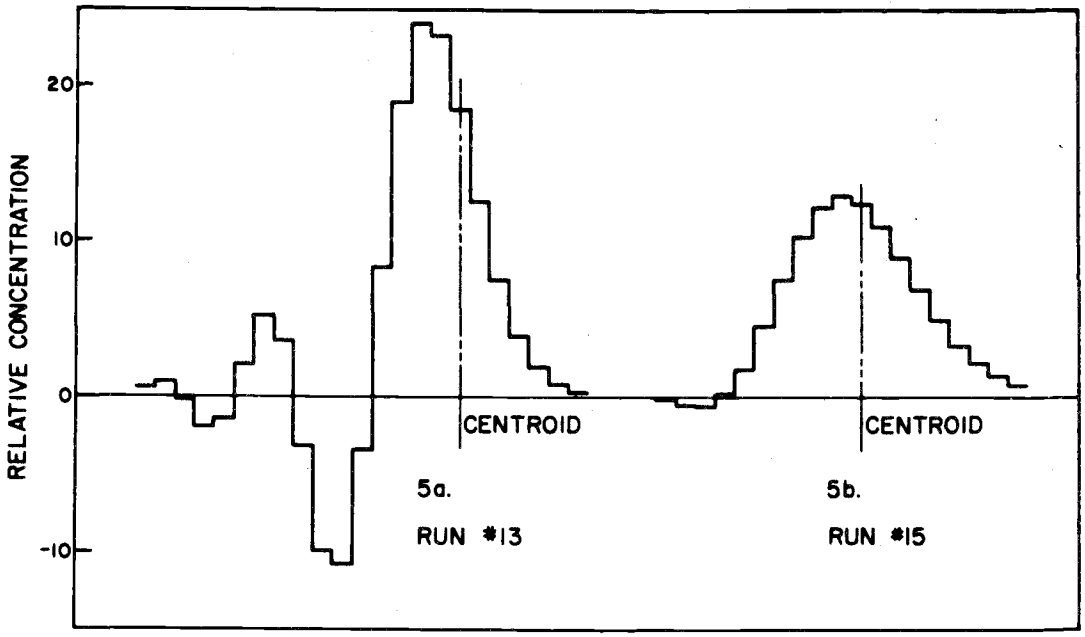

Figure 11. Concentration distributions for runs number 13 and 15.

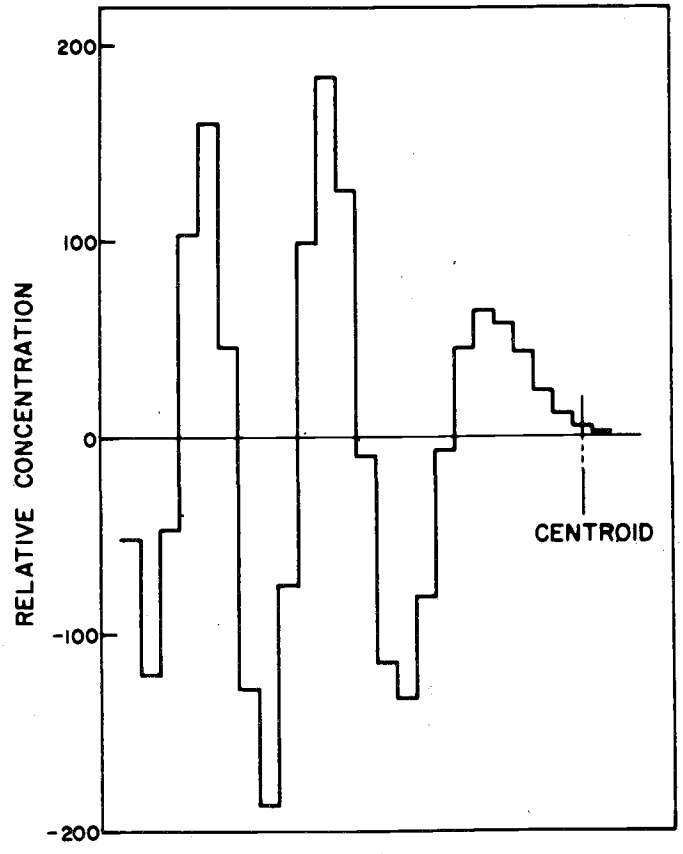

Figure 12. Concentration distribution for run number 17.

Calculating the Dispersion Error

Consider the convection of a single slug load as shown in Figure 8. As a continuous distribution may be visualized in finite-difference terms as a series of slug loads (Figure 7) the derivation of the pseudo dispersion coefficient will involve the convection of a single slug. This general approach simplifies the derivation and allows for the variation of pseudo dispersion with distance that might occur with more complex models. Referring to Figure 8 and Equation 19, the variance of the distribution at time T is:

$$\delta^2_{(T)} = C_{(N, T)}\Delta x^3/12 C_{(N, T)}\Delta x = \Delta x^2/12 \qquad (21)$$

The variance at time $T + \Delta T$ can similarily be determined by noting:

$$C_{(N, T+\Delta T)} = C_{(N, T)} + \gamma C_{(N, T)}\left(\frac{U\Delta T}{\Delta x}\right) - (1-\gamma)C_{(N, T)}\left(\frac{U\Delta T}{\Delta x}\right) \qquad (22)$$

$$C_{(N-1, T+\Delta T)} = -\gamma C_{(N, T)}\left(\frac{U\Delta T}{\Delta x}\right) \qquad (23)$$

$$C_{(N+1, T+\Delta T)} = (1-\gamma)C_{(N, T)}\left(\frac{U\Delta T}{\Delta x}\right) \qquad (24)$$

and substituting into Equation 19. The result after reduction is:

$$\delta^2_{(T+\Delta T)} = \frac{\Delta x^2}{12} + U\Delta T\Delta x - (U\Delta T)^2 - 2\gamma U\Delta T\Delta x \qquad (25)$$

Defining pseudo dispersion D_p as one-half the rate change in

variance leads to:

$$D_p = \frac{\delta^2(T+\Delta T) - \delta^2(T)}{\Delta T} \qquad (26)$$

Substituting Equations 21 and 25 into Equation 26 results in:

$$D_p = \frac{U}{2}[(1-2\gamma)\Delta x - U\Delta T] \qquad (27)$$

Equation 27 defines the spreading error associated with the general numerical convection equation, Equation 15. Results of Equation 27 given in column (9) of Table 2 agree exactly with the dispersion errors listed in column (6).

Substitution of $\gamma = 0$ into Equation 27 leads to Equation 13. Equation 13 was originally obtained through a mixing length description of dispersion and a visualization of numerical convection similar to that shown in Figure 8

Substitution of $\gamma = 0.5$ into Equation 27 leads to

$$D_p = -\frac{U^2\Delta T}{2}$$

which is identical in magnitude to Equation 14 given by Prych (1969) but opposite in sign.

Figure 13 shows the manner in which D_p varies with U, Δx, ΔT and γ. The backward difference equation ($\gamma = 0.00$) always results in a positive value of D_p while the central and forward difference equations always result in negative values of D_p. The quarter

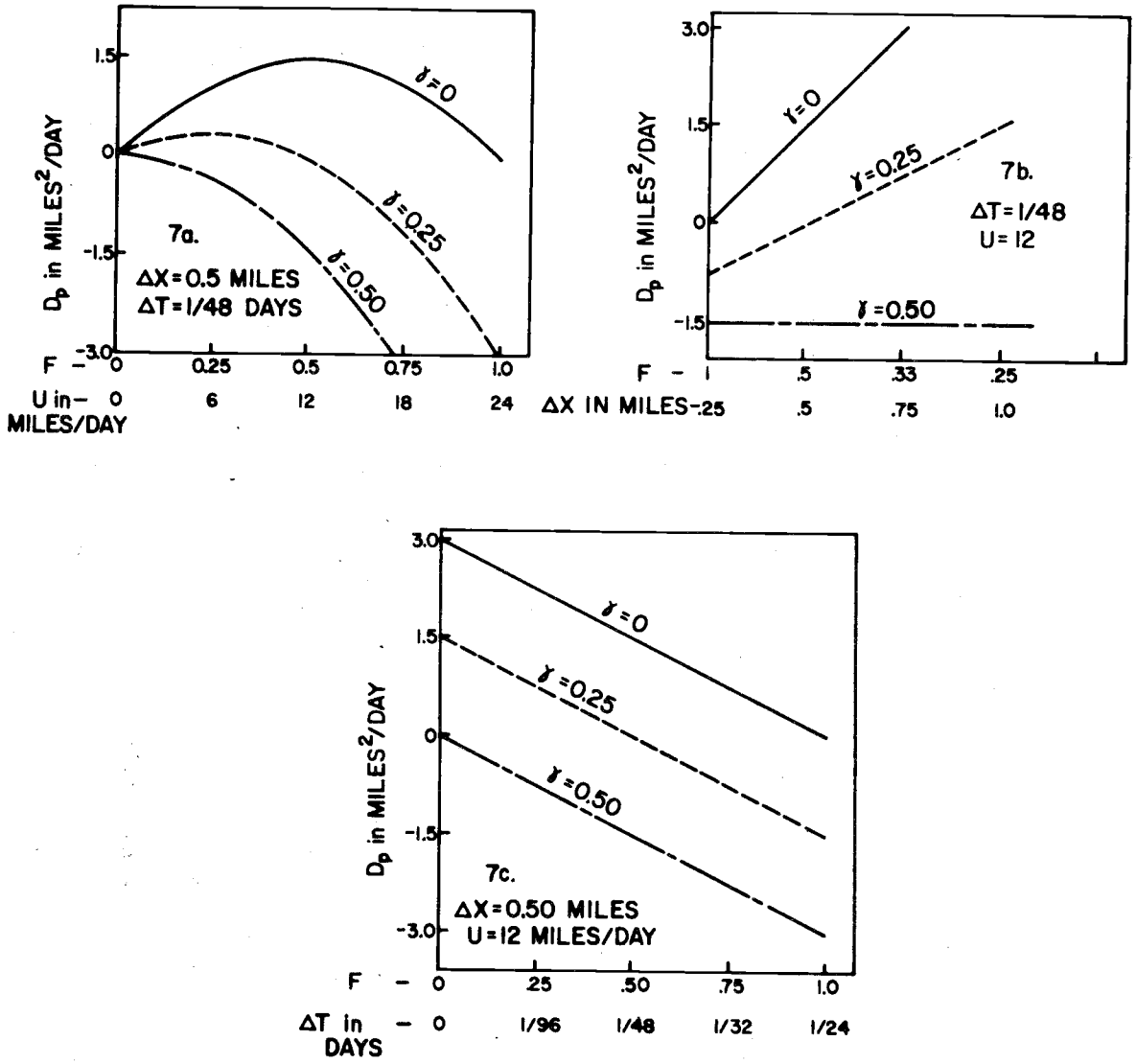

Figure 13. Pseudo dispersion as a function of U, ΔT, ΔX and γ.

point equation may result in a positive or negative value of D_p depending on the values of Δx, ΔT and U.

Numerical Convection Error

While results shown in Table 2 demonstrate that Equation 27 can satisfactorily describe the dispersion error, it is desirable to know under what conditions Equation 27 can be a suitable estimate of the total errors associated with numerical convection Equation 15.

In order to determine how well Equation 27 describes the total convection error, numerical results from Equation 15 were compared to analytical solutions of Equation 20 in which $D_p = D$ and initial conditions are identical. For the initial condition shown in Figure 9a, the analytical solution to Equation 20 with suitable boundary conditions is:

$$C = \frac{C_0}{2}\left[\operatorname{erf}\left(\frac{\Delta x/2 - Z}{2\sqrt{DT}}\right) + \operatorname{erf}\left(\frac{\Delta x/2 + Z}{2\sqrt{DT}}\right)\right] \qquad (28)$$

where C_0 = the initial concentration, D = the dispersion coefficient, T = time from injection of the slug load, and Z = the distance from the centroid to C (Carslaw and Jaeger, 1959).

Figure 9b shows the distribution calculated by Equation 28 with D = 0.5625 superimposed on the distribution obtained by Equation 15 for the same parameters. Three methods for defining the maximum difference between these curves were considered. These methods are:

1. the maximum distance between two ordinates at a point along the X axis (length a on Figure 9b).
2. the maximum ratio obtained by dividing the difference in ordinates at a point along the X axis by the ordinate of the analytical solution (a/b on Figure 9b), and
3. the maximum difference between two ordinates at a point along the X axis divided by the maximum ordinate of the analytical solution (a/c on Figure 9b).

The first definition does not indicate a relative magnitude and the second is always greatest in the tail of the distribution where the denominator becomes very small. Therefore, the third definition was adopted as the most meaningful indicator of the maximum discrepancy between the two curves. The discrepancy in Figure 9b is:

$$\epsilon = \frac{6.28}{18.63} \times 100 = 33.7\% \qquad (29)$$

It was observed that the magnitude of the discrepancy decreased with time for all cases tested with positive D_p. An example of these results is shown in Figure 14. The discrepancy was observed to be large and to increase with time for negative values of D_p except at very small values of F.

It can be seen by examining Equation 15 that for a slug load as in Figure 8 and a specific γ, the concentration at the end of a time increment, $C_{(N,\ T+\Delta T)}$, will always be the same for a particular value

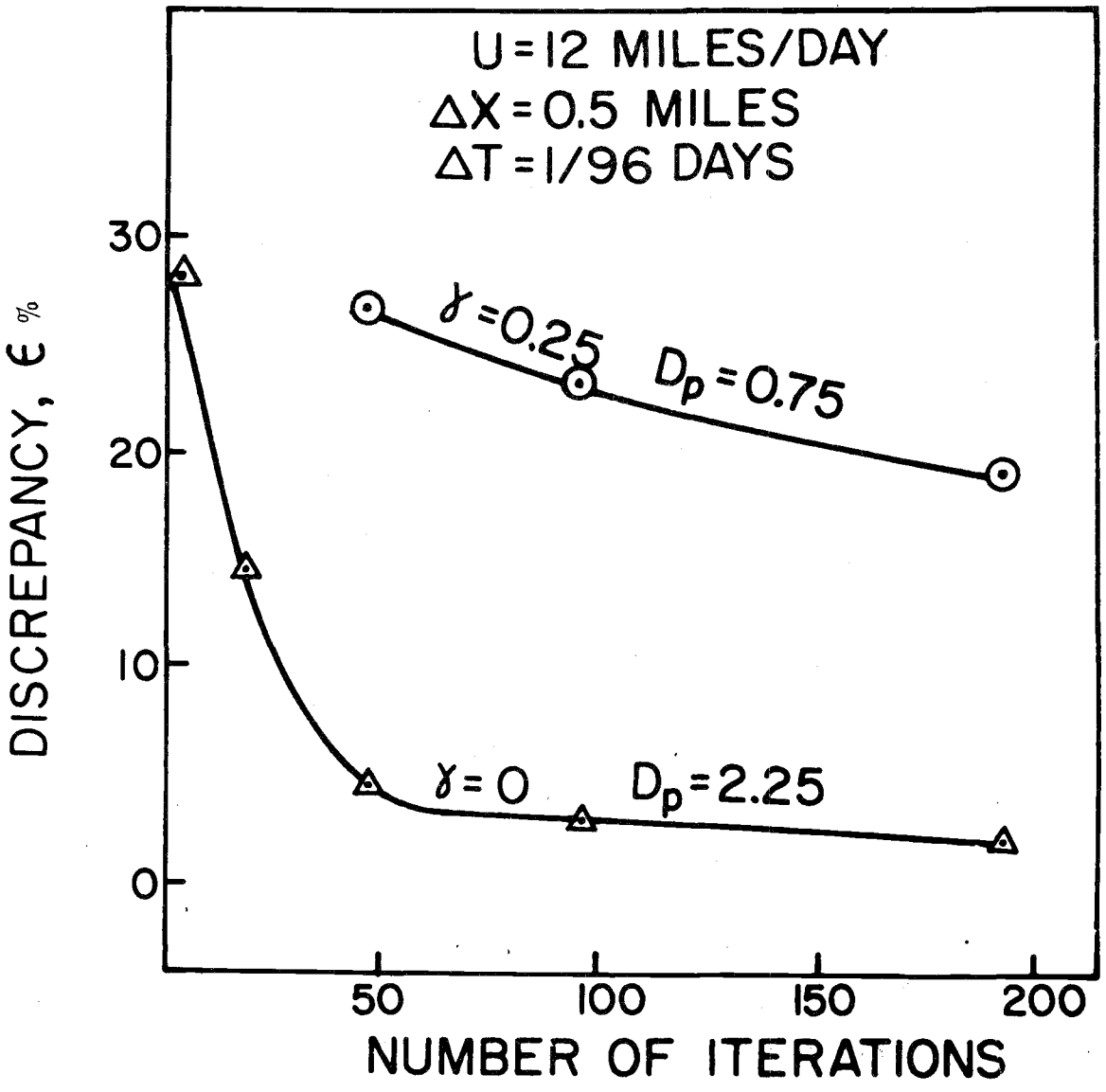

Figure 14. Reduction of ϵ with time.

of F. Thus, the concentration in a particular cell after a specific number of iterations will always be the same for a given value of F and γ no matter what individual values of Δx, ΔT and U are used to make up the F ratio. In Equation 28 let $Z = n\Delta X$, $T = k\Delta T$ and $D = \frac{U}{2}[(1-2\gamma)\Delta x - U\Delta T]$ where n = number of increments away from centroid and k = number of iterations. Rearranging and combining terms lead to:

$$C = \frac{C_0}{2}\left[\operatorname{erf}\left(\frac{1/2 + n}{\sqrt{2k}\sqrt{(1-2\gamma)F - F^2}}\right) + \operatorname{erf}\left(\frac{1/2 - n}{\sqrt{2k}\sqrt{(1-2\gamma)F - F^2}}\right)\right]$$

Since for a particular segment after a specific number of iterations and a given value for γ, both the analytical and difference equation are solely dependent on the value of F, the discrepancy as previously defined can be plotted as a function of F as shown in Figure 15.

Equation 27 accurately describe the total convection errors for the backwards difference method as shown by the low discrepancies shown in Figure 15. The discrepancies were least when F = 0.5 which is the region of maximum dispersion error (see Figure 13).

Oscillations were so great in the central and downstream difference results that no attempt was made to quantify these discrepancies.

Discrepancies were least for the quarter point method at low values of F, though all discrepancies were considerably higher than those observed for the backward difference method.

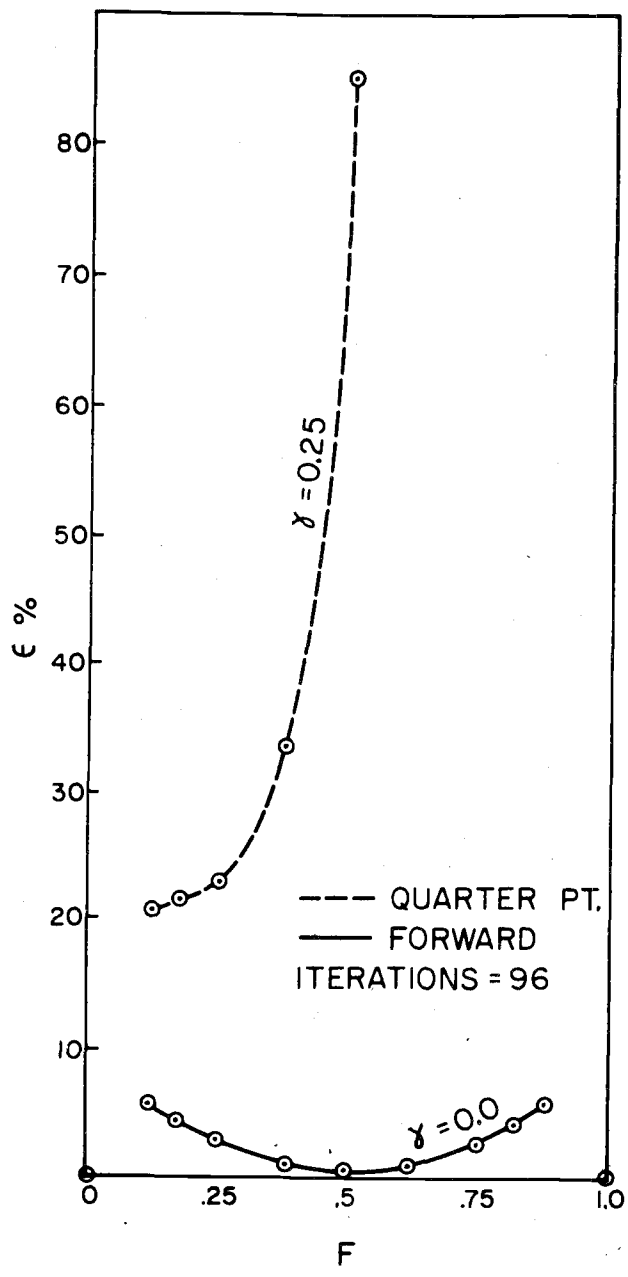

Figure 15. Comparison of ϵ for the quarter point and upstream difference equations.

Control of Finite-Difference Errors

The general method of controlling finite-difference convection errors involves first selecting a method for which most of the numerical error can be described in a pseudo dispersion coefficient. The actual dispersion being modeled in addition to convection is then reduced by an amount equal to the pseudo-dispersion. Thus, the pseudo dispersion coefficient plus the dispersion coefficient used in the numerical computations of dispersion equal the desired dispersion being modeled. This general method has been discussed by Bella and Dobbins (1968). If high accuracy need be assured it is desirable, though not always necessary, to select Δx and ΔT so that the actual dispersion being simulated by the entire model is greater than the dispersion error of the convection portion given by Equation 27.

Convection and dispersion of a slug load were numerically simulated using this method of error correction. The distributions resulting from these runs were compared to the analytical solutions and the discrepancy, as previously defined, was determined. The numerical method of including dispersion has been previously given by Bella and Dobbins (1968). Table 3 indicates the discrepancies associated with various values of U and γ for the specific conditions: $\Delta x = 0.5$ miles, $\Delta T = 1/96$ days, $D = 1.5$ miles^2/day and $T = 2$ days. During each run the actual rate change in variance of the distribution was

Table 3. Comparison of discrepancies associated with several numerical schemes.

		γ			
(Miles/day)	F	0.00	0.25	0.50	1.00
6	0.125	ϵ = 3.2	4.2	5.0	6.5
		Dp = 1.31	0.56	- .19	-1.69
12	0.250	ϵ = 3.7	7.2	10.4	*
		Dp = 2.25	0.75	-0.75	-3.75
24	0.500	ϵ = 1.0	13.3	22.4	**
		Dp = 3.00	0.00	-3.00	-9.00
36	0.750	ϵ = 3.7	22.0	33.6	**
		Dp = 2.25	-2.25	-6.75	-15.75
46	0.958	ϵ = 1.6	30.5	**	**
		Dp = 0.48	-5.27	-11.02	-22.52

Δx = 0.5 miles, ΔT = 1/96 days, D = 1.5 miles^2/day and T = 2 days.

** Severe oscillations * Not measured

exactly equal to twice the desired dispersion coefficient, D.

The results shown in Table 3 demonstrate that the errors are best controlled when the backward difference method is used, even when $D_p > D$. The quarter point method gives reasonable results when F is low as was indicated previously in Figure 15.

The central and forward difference methods were best when convection was low and thus when dispersion could dominate the results.

MODEL APPLICATION

General

Pollution concentrations resulting from continuous loadings present special problems when the receiving water body is influenced by tidal action. For example, the water resting over the outfall during slack water will pick up more pollutant than water traveling at relatively high velocity at other times during the tidal cycle. The volume of water passing a given station in a unit of time and, therefore, the dilution capacity of the stream is continuously changing. Hence, the concentration distribution in the channel will be characterized by a series of peaks all moving up and down the channel with the tidal fluctuations. The maximum concentration would be expected to occur at low water slack. The distance between peaks will be dependent on the net convection during each tidal cycle due to fresh water inflow. The magnitude of the concentration peaks will be diminished in time in accordance with the dispersion characteristics of the particular estuary and the decay rate of the pollutant. They can be reduced initially at the outfall by varying the rate of pollutant addition so that it is proportional to stream velocities.

These localized maxima may be the critical concentrations in the estuary. They may form a series of barriers against migrating fish or exceed the toxicity threshold levels of other aquatic organisms.

These peaks could have a detrimental effect on the estuary biota which would not be predicted if only average concentrations based on the tidal prism were considered. The peak concentrations caused by slack water buildup must, therefore, be considered when predicting the impact of a new pollutant source on an established ecosystem.

A dye study was conducted in the upper reach of the Yaquina Estuary in order to demonstrate the magnitude of slack water buildup and to provide field data to compare with the computer model.

Field Study

The study area was a fairly uniform seven mile section of channel between Elk City and Mill Creek without intersecting tributaries or mud flats. Dye was injected into the channel at a point approximately one mile down the Estuary from Elk City. A diffuser was constructed by placing six nozzles at equal spacing on a 150 foot length of half inch plastic irrigation pipe. The nozzles were adjusted to provide equal flow rates before installing the diffuser across the estuary channel. The diffuser was anchored to the bottom by concrete blocks and floats were attached in order to keep the nozzles approximately one foot above the bottom. Water was pumped into the diffuser at a rate of about 20 gallons per minute. A concentrated solution of rhodamine-B dye was injected into the diffuser at a nearly constant rate of 0.2 pounds per hour for 12 hours .

Buoys were set to divide the stream width into quarters at the diffuser and at sections 235 feet on both sides of the diffuser. Samples were taken near each of the buoys at the diffuser and at the downstream section every half hour or as determined necessary. Samplers were constructed of long poles with rubber bulbs attached at various heights so that four to six samples could be taken simultaneously at different depths. Each solid vertical line in Figure 16 shows the arithmetic average of the vertical samples taken near each buoy at the diffuser. The dash lines represent similar values for the downstream section. The actual concentrations varied between zero and three parts per billion.

Velocities were measured at four depths near each of the quarter points of the stream width near the diffuser. An arithmetic average of the 12 velocity measurements was assumed to represent the average cross section velocity. These values are shown on Figure 17. After 21:00 hours, velocity measurements were taken only at the channel center.

Water surface elevations were continuously measured with Stevens automatic tide recorders at Elk City and at Mill Creek. Elevations at the diffuser were measured at the same time that velocities were recorded. Observed data are shown in Figures 18, 19 and 20.

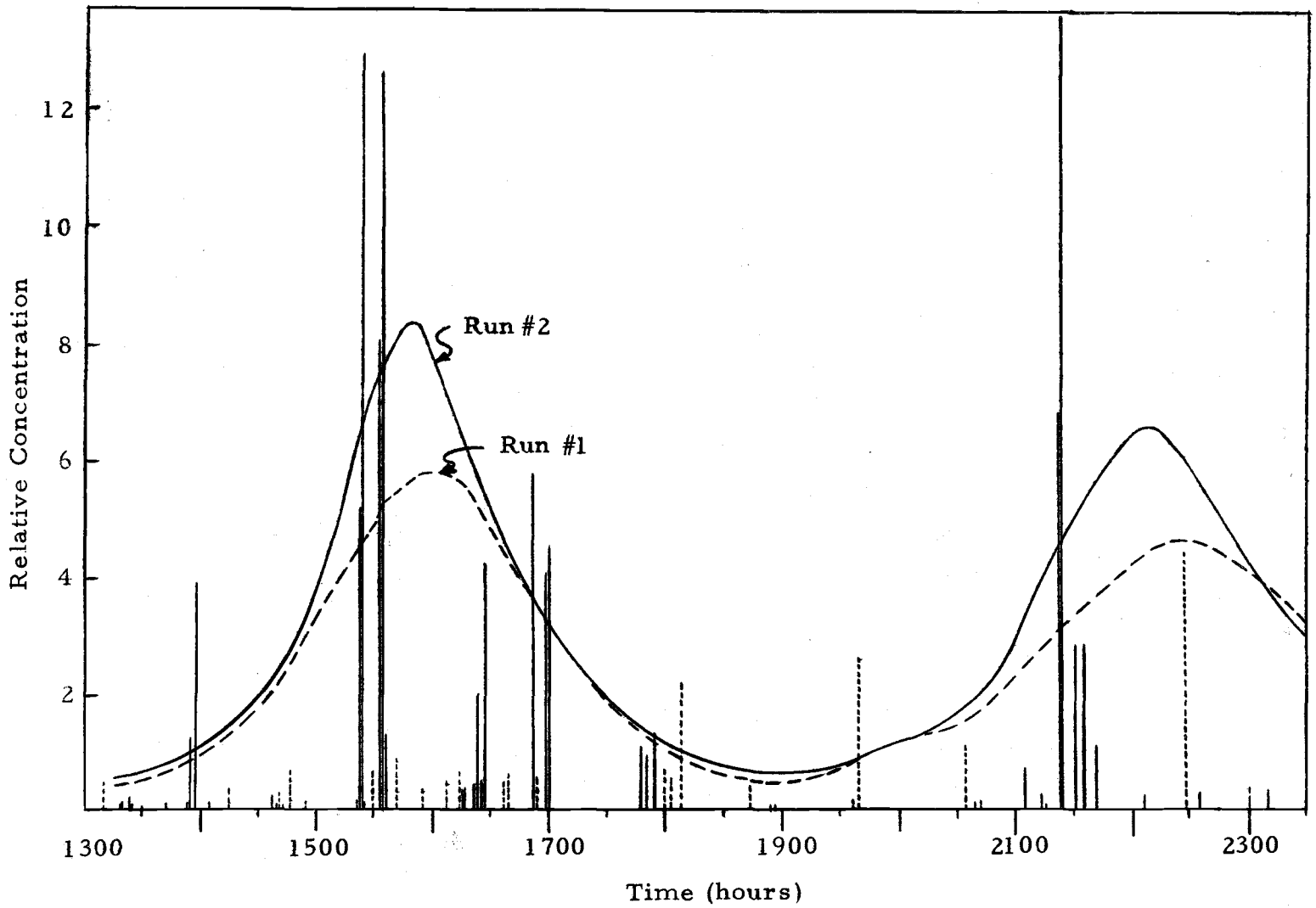

Figure 16. Dye tracer study on Yaquina Estuary.

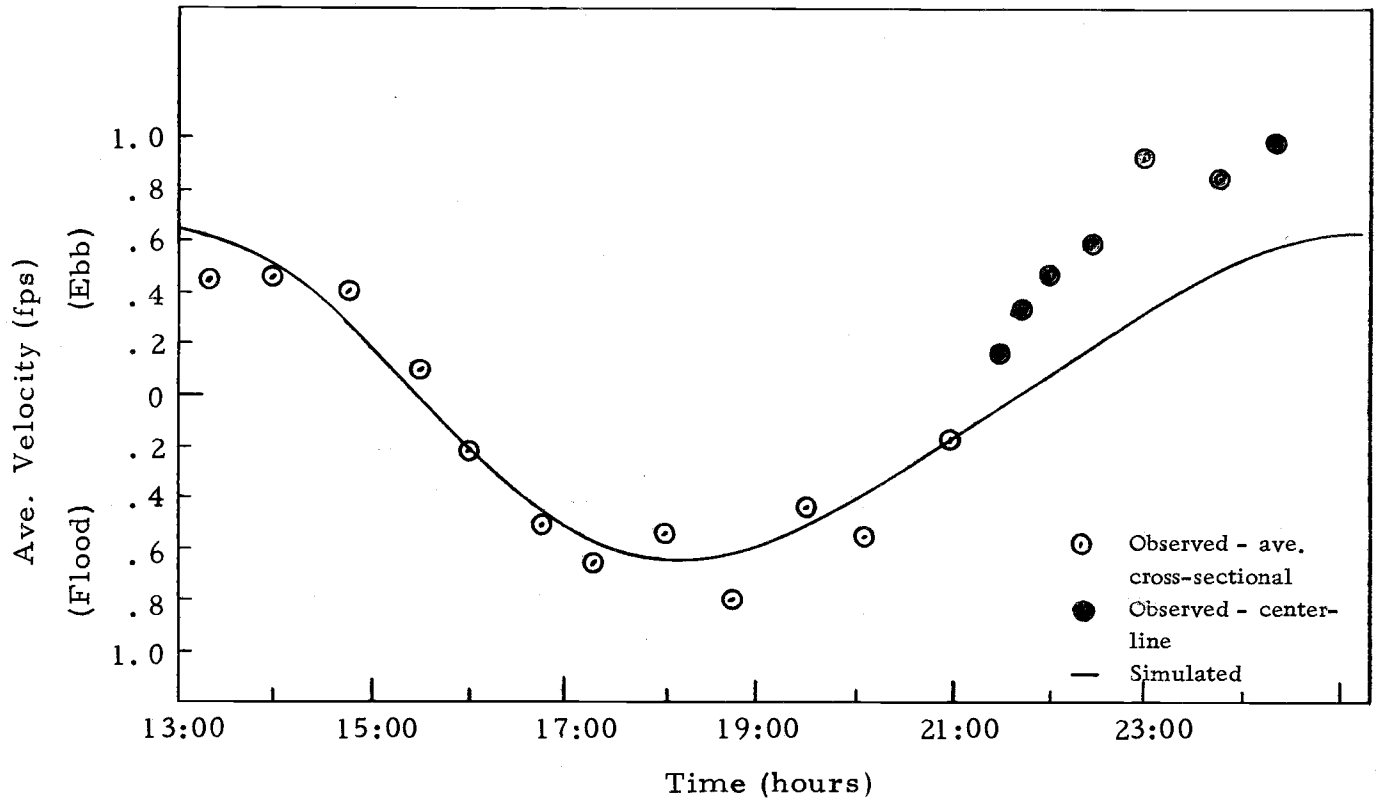

Figure 17. Observed and simulated velocities at the diffuser section.

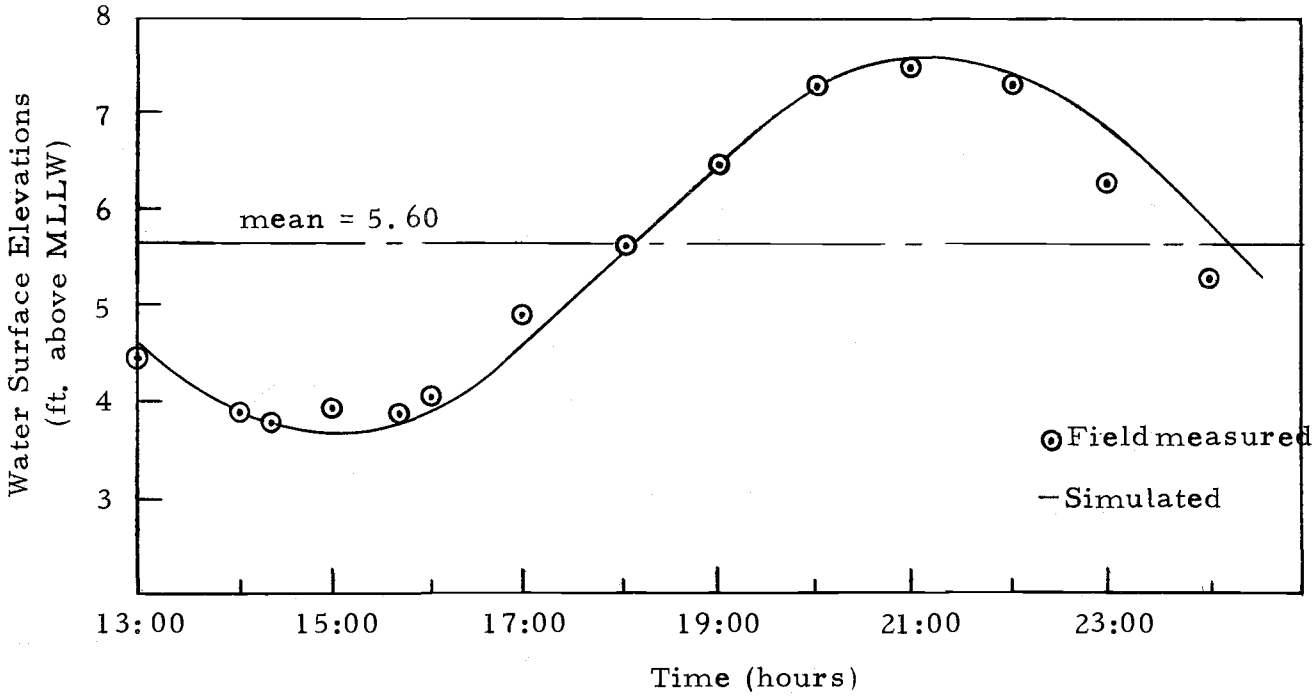

Figure 18. Water surface elevations at Mill Creek.

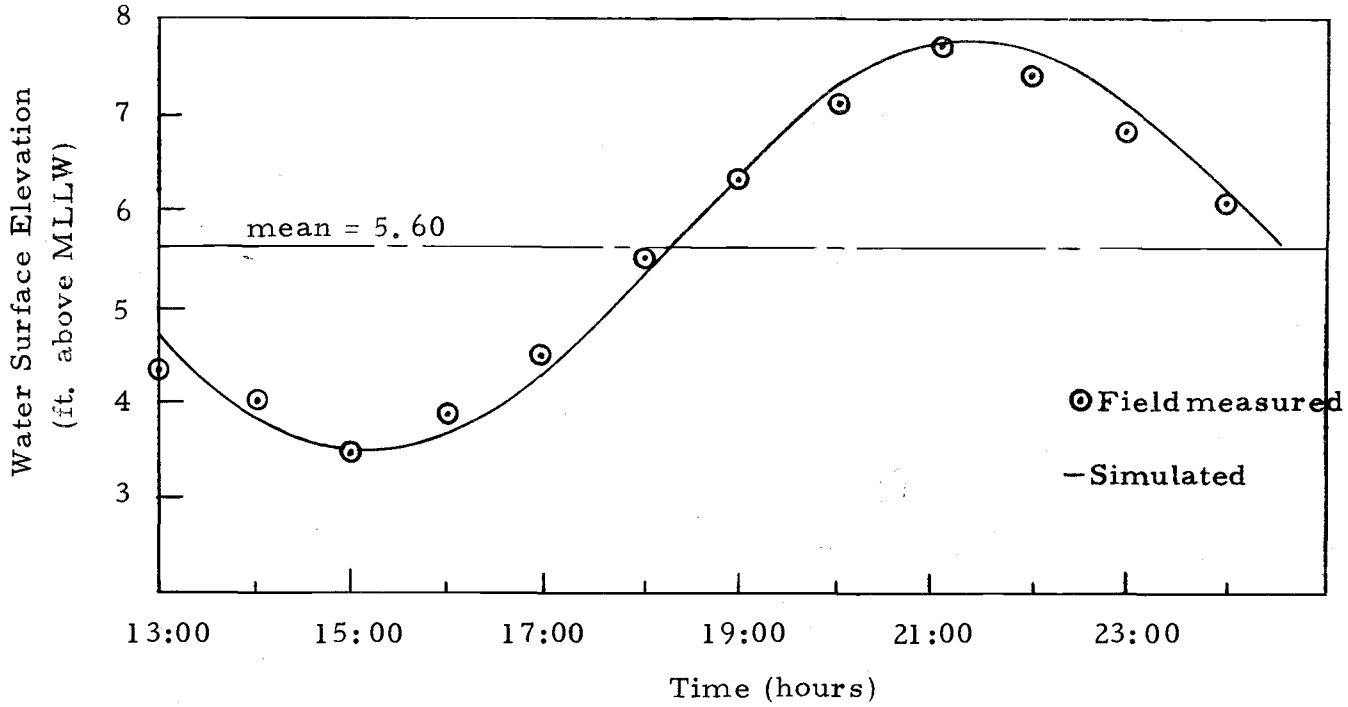

Figure 19. Water surface elevations at Elk City.

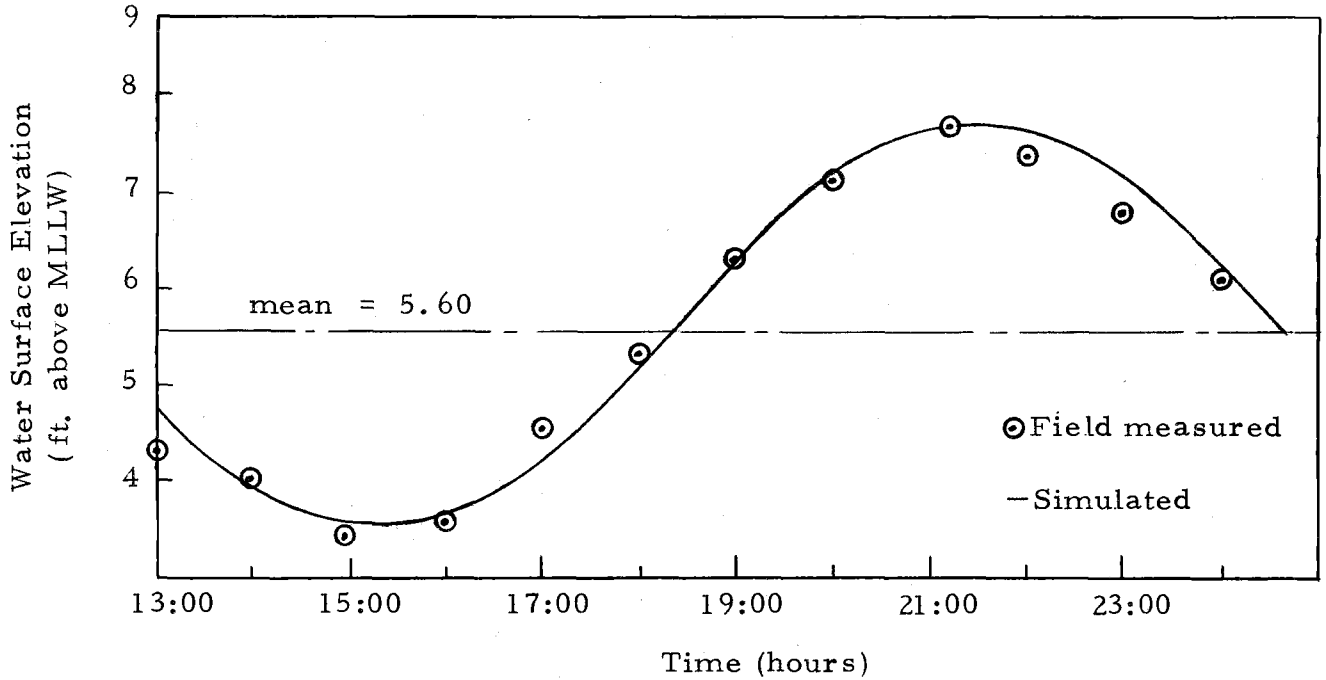

Figure 20. Water surface elevations at diffuser section.

Computer Simulation

The mean tidal elevation during the study period was determined to be 5.6 feet above mean low low water (MLLW) from Figures 18, 19 and 20. Channel cross section dimensions were obtained (Goodwin, Emmett and Glenne, 1970) and cross section areas were calculated for the mean water surface elevation. This data was approximated by algebraic functions for the computer simulation as shown in Figures 21 and 22. Values above Elk City were estimated from cursory field observations.

A study of tidal hydraulics in the Yaquina Estuary (Goodwin, Emmett and Glenne, 1970) indicated that the end of the estuary could be approximated at a point 3.9 miles from Elk City for the particular tidal conditions during the study. A completely reflecting boundary ($\beta = 1.0$) was assumed at the end of the Estuary because actual tidal velocities and water surface elevations were observed to be ninety degrees out of phase. Values for k and μ were estimated emperically by methods developed by Ippen (1966) for a uniform rectangular channel. These values were adjusted slightly by trial and error in order to obtain a good fit between output from the water quantity model and observed data. The resulting values were $k = 0.0482$ radians per mile and $\mu = 0.0219$ per mile. Computer results and field data are shown on Figures 18 through 20.

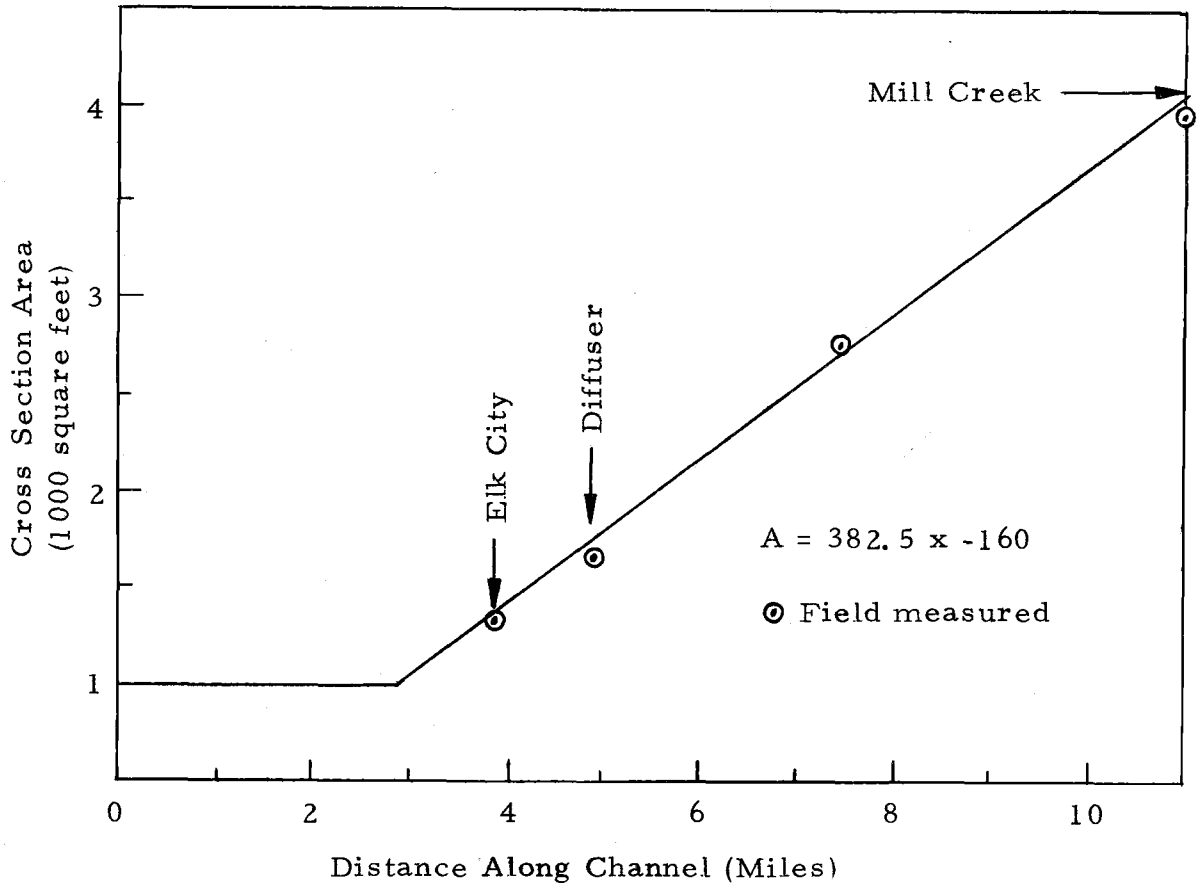

Figure 21. Function representing channel areas.

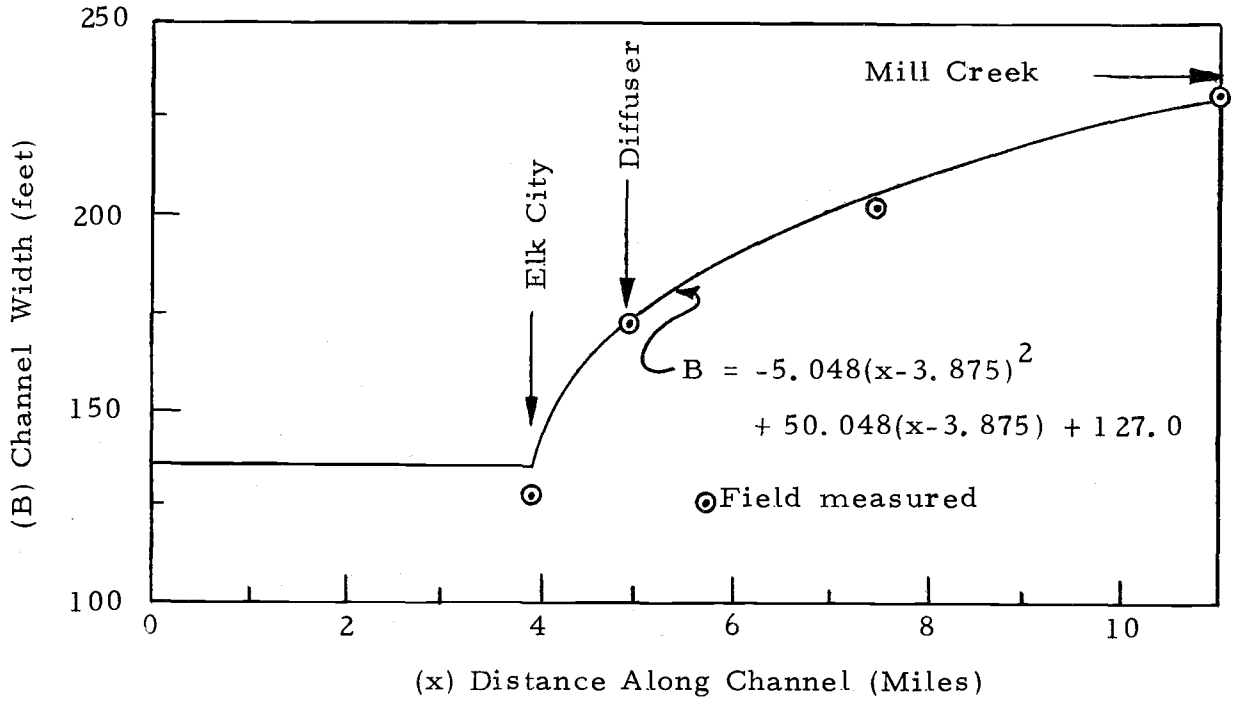

Figure 22. Function representing channel widths.

The channel segment length (Δx) and the time increment (ΔT) were selected as 0.10 miles and 1/6 hour respectively. These grid parameters were in the range which produced good accuracy for the water quantity model as indicated in Table 1. They also provided reasonably low values of pseudo dispersion as shown on Figure 23.

No values for the dispersion coefficient (D), as defined in this model, were available for the Yaquina Estuary. However, results from the field study, Figure 16, indicated steep gradients in the tracer concentration. Therefore, D was selected as low as possible but large enough to maintain a positive net dispersion coefficient at all times during the tidal cycle. Run number one was conducted using a constant dispersion coefficient equal to 75 feet^2/sec. (0.218 miles^2/day). Run number two used a dispersion coefficient which varied as a linear function of the velocity. The maximum value for the variable dispersion coefficient was obtained by equating the area under the two curves shown on Figure 23.

Discussion

The water quantity model represented the observed data reasonably well as indicated on Figures 17 through 20.

The observed average cross-sectional velocities during ebb tide between 13:00 and 15:00 ranged from 83.5% to 93.7% of the velocities at channel center. The departure of the model from the prototype in

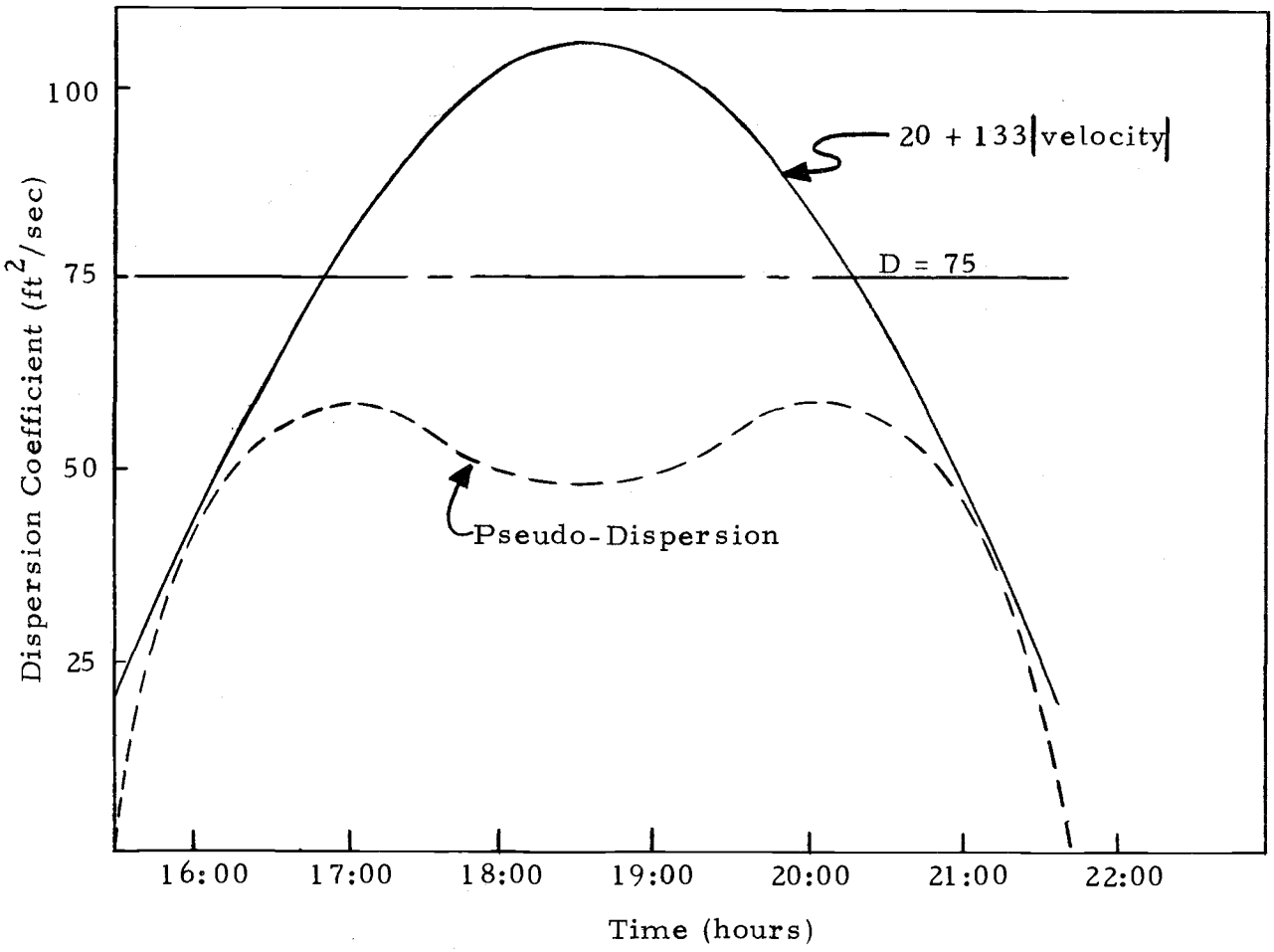

Figure 23. Dispersion coefficients for one half of a tidal cycle at the diffuser.

Figure 17 may be partially explained by the fact that velocity measurements were taken only at the channel center after 21:00 hours and, therefore, are higher than the average cross-sectional velocities represented by the model. A method was considered to estimate average velocities for the period after 21:00 hours by correlating the two ebb tides. However, cross-sectional areas for the two periods differ by as much as 40% and maximum velocities appear to shift across the channel at various tidal heights so it was determined unrealistic to attempt to adjust the observed values after 21:00 hours. The fact that the observed data could be approximated by varying only two parameters would tend to indicate that the model possesses a significant relationship to the prototype. However, the study by Goodwin, Emmett and Glenne (1969) indicates that k and μ would have to be represented as functions of distance and water surface elevation for runs longer than one tidal cycle with irregular tidal wave amplitudes. Emperical determination of these functions would be extremely difficult.

Comparison of runs number one and two in Figure 16 indicates that the variable dispersion coefficient causes the steepest concentration gradients and provides the best approximation to the observed data. This result is consistent with the common sense concept that dispersion is related to stream velocity. The concentrations from the simulated runs consistently underestimated the maximum observed

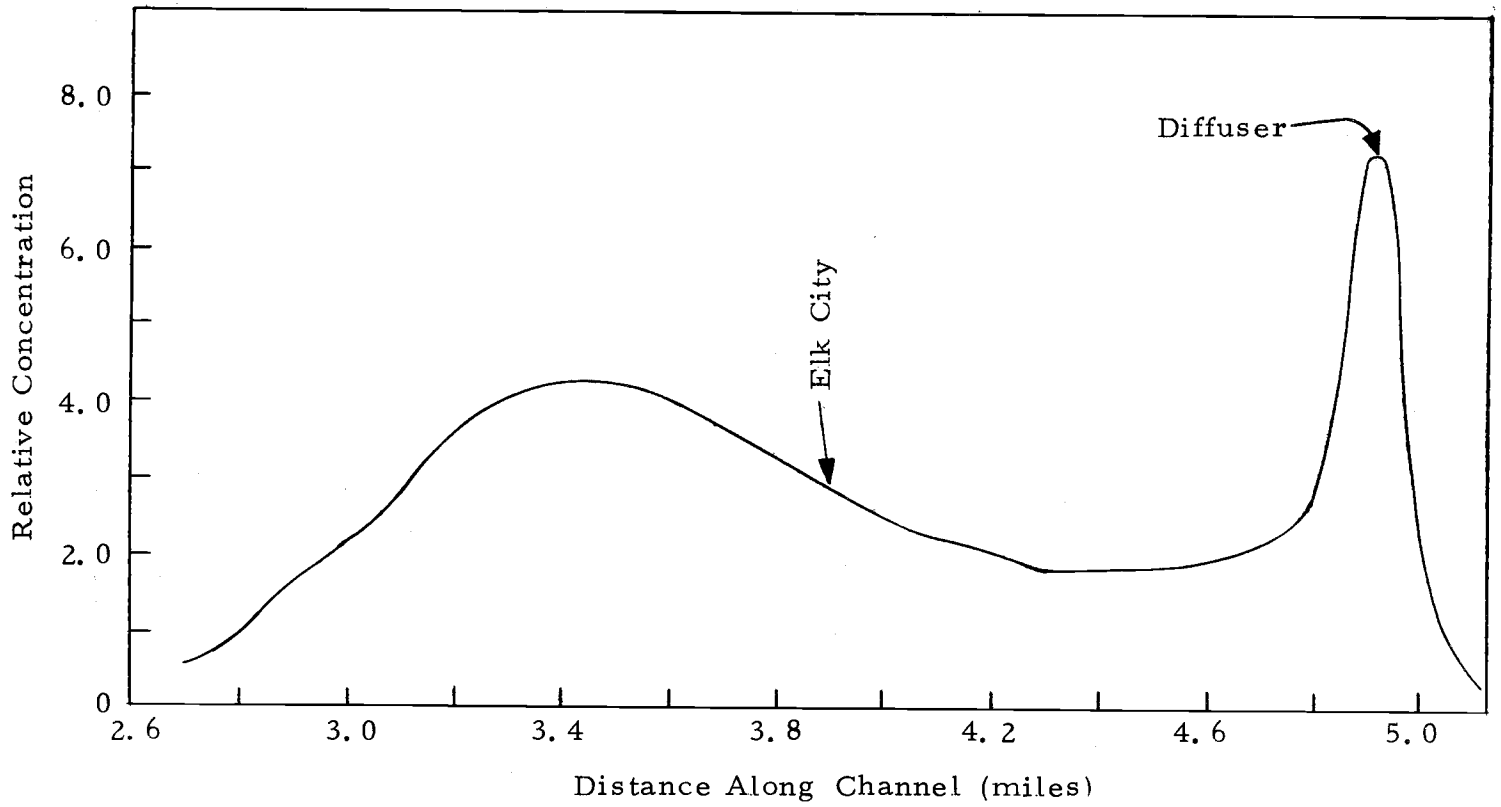

Figure 24. Tracer concentrations along the channel, from computer run number two at 22:10 hours.

values. This trend was expected, however, because the finite-difference representation in the model calculates values averaged over the distance Δx. The time of occurrence of the simulated peaks lagged the observed values, although run number two was slightly earlier than run number one. This lag might also be attributable to the averaging effect of the finite-difference scheme.

Figure 24 shows the tracer distribution along the channel calculated by run number two at 22:10 hours. The two slack water peaks and the spreading of the first peak due to dispersion are apparent on the figure.

The wide scatter of observed data in Figure 16 indicates that the tracer was not well mixed throughout the cross section area and, therefore, that the estuary was not one dimensional as assumed. Part of the scatter may have been eliminated by using a diffuser with more ports. Using a larger quantity of dye in order to obtain maximum concentrations in the neighborhood of 0.5 parts per million would provide greater precision in sampling and sample measurement. The results do, however, give a good indication of the relative magnitude of slack water buildup and demonstrate the necessity for considering these peak concentrations when predicting the impact of pollution outfalls on the environment.

SUMMARY AND CONCLUSIONS

A one-dimensional model was developed which simulates the distribution of a dissolved pollutant in an estuary. Finite-difference methods were utilized on a digital computer to yield solution in terms of time and longitudinal distance. Methods were developed for calculating tidal velocities at any point in the estuary as a function of the tide at the mouth.

Errors associated with finite-difference convection were investigated. The errors associated with the model were classified into three categories: oscillation errors, skewness errors, and dispersive errors. Errors were most noticeable for computations of slug load convection. Smooth distribution computations tended to hide errors and were thus poor tests of numerical methods.

A means of accurately calculating the dispersion error was developed. Numerical methods in which most of the error was classified as a dispersive error were investigated. It was then shown that the error associated with such methods could be qualified and controlled.

A diffuser was installed at the Yaquina Estuary, Newport, Oregon and dye was released at a constant rate for 12 hours. Both field and simulated data indicated that steep concentration gradients could occur in the vicinity of the outfall during slack water periods.

BIBLIOGRAPHY

Asano, Takashi. 1967. Distribution of pollutional loadings in Suisun Bay. National Symposium on Estuarine Pollution, Stanford University August 1967. Stanford, California. p. 441-461.

Carslaw, H. S. and J. C. Jaeger. 1959. Conduction of heat in solids. London, Oxford University Press. 530 p.

Bain, Richard C. 1968. Predicting DO variations caused by algae. Journal of the Sanitary Engineering Division, American Society of Civil Engineers 94:867-881.

Bella, David A. 1968. Discussion of solution of estuary problems and network programs by J. V. Leeds and H. H. Bybee. Journal of the Sanitary Engineering Division, American Society of Civil Engineers 94:180-181.

Bella, David A. and William Dobbins. 1968. Difference modeling of stream pollution. Journal of the Sanitary Engineering Division, American Society of Civil Engineers 94:995-1016.

Clark, Shirley M. and George R. Snyder. 1969. Timing and extent of a flow reversal in the lower Columbia River. Limnology and Oceanography 14:960-965.

Dresnack, Robert and William E. Dobbins. 1968. Numerical Analysis of BOD and DO profiles. Journal of the Sanitary Engineering Division, American Society of Civil Engineers 94:789-807.

Dornhelm Richard B. and David A. Woolhiser. 1968. Digital Simulation of estuarine water quality. Water Resources Research 4:1317-1328.

Fisher, Hugo B. 1966. A note on one-dimensional dispersion model. Air and Water Pollution International Journal 10:443-452.

Fisher, Hugo B. 1969. A lagrangian method for predicting dispersion in Bolinas Lagoon, California. Menlo Park, California. 1969. (United States Department of the Interior, Geological Survey, Water Resources Division) (Open-File Report).

Glenne, Bard. 1969. Assistant Professor, Oregon State University, Dept. of Civil Engineering. Class lecture. Corvallis, Oregon.

Goodwin, C. R, E. W. Emmett and Bard Glenne. 1970. Tidal study of three Oregon estuaries. 32p. (Oregon State University Engineering Experiment Station. Bulletin No. 45)

Harleman, Donald R., Chok-hung Lee, and L. C. Hall. 1968. Numerical studies of unsteady dispersion in estuaries. Journal of the Sanitary Engineering Division, American Society of Civil Engineers 94:897-911.

Holley, Edward R. 1969. Discussion of difference modeling of stream pollution by David A. Bella and William E. Dobbins. Journal of the Sanitary Engineering Division, American Society of Civil Engineers 95:968-972.

Ippen, A. T. 1966. Estuary and coastline hydrodynamics. New York, McGraw-Hill. 744 p.

Leeds, J. V. and H. H. Bybee. 1967. Solution of estuary problems and network programs. Journal of the Sanitary Engineering Division, American Society of Civil Engineers 93:29-36.

O'Connor, Donald J. 1960. Oxygen balance of an estuary. Journal of the Sanitary Engineering Division, American Society of Civil Engineers 86:35-55.

O'Connor, Donald J. 1965. Estuarine distribution of non-conservative substances. Journal of the Sanitary Engineering Division, American Society of Civil Engineers 91:23-42.

O'Connor, Donald J., John St. John, and Dominic M. DiToro. 1968. Water quality analysis of the Delaware River Estuary. Journal of the Sanitary Engineering Division, American Society of Civil Engineers 94:1225-1252.

Orlob, G. T., R. P. Shubinski and K. D. Feigner. 1967. Mathematical modeling of water quality. National Symposium on Estuarine Pollution, Stanford University. August 1967. Stanford, California p. 646-675.

Pence, George D., John Jeglic, and Robert Thomann. 1968. Time-varying dissolved-oxygen model. Journal of the Sanitary Engineering Division, American Society of Civil Engineers 94: 381-401.

Prych, E. A., and R. E. Chidley. 1969. Discussion of numerical studies of unsteady dispersion in estuaries. Journal of the Sanitary Engineering Division, American Society of Civil Engineers 94:897-911.

Thayer, Richard P. and Richard G. Krutchkoff. 1967. Stochastic model for BOD and DO in streams. Journal of the Sanitary Engineering Division, American Society of Civil Engineers 93: 59-72.

Thomann, Robert V. 1963. Mathematical model for dissolved oxygen. Journal of the Sanitary Engineering Division, American Society of Civil Engineers 89:1-30.

Thomann, Robert V. 1967. Time-series analysis of water-quality data. Journal of the Sanitary Engineering Division, American Society of Civil Engineers 93:1-23.

Wastler, T. A. and Carl M. Walter. 1968. Statistical approach to estuarine behavior. Journal of the Sanitary Engineering Division, American Society of Civil Engineers 94:1175-1193.

Welty, James R. 1969. Thermal plume dispersion-a computer model. Water Studies in Oregon, Oregon State University Water Research Institute. Corvallis, Oregon. p. 69-85.